Supporting Information

Fluorescence-Plane Polarization for the Real-Time Monitoring of Transferase Migration in Living Cells

Yafu Wang,[a] Huiyu Niu,[a] Kui Wang,[a] Liu Yang,[a] Ge Wang,[d] Tony D. James,[a c] Jiangli Fan[*b] and Hua Zhang[*a]

[a] Collaborative Innovation Centre of Henan Province for Green Manufacturing of Fine Chemicals; Key Laboratory of Green Chemical Media and Reactions, Ministry of Education; Henan Key Laboratory of Organic Functional Molecule and Drug Innovation; School of Chemistry and Chemical Engineering, Henan Normal University, Xinxiang, Henan 453007, P. R. China;

[b] State Key Laboratory of Fine Chemicals; Frontiers Science Center for Smart Materials, Oriented Chemical Engineering; School of Chemical Engineering, Dalian University of Technology, Dalian, Liaoning 116024, P. R. China;

[c] Department of Chemistry, University of Bath, Bath, BA2 7AY, UK;

[d] Xinxiang Medical University, Xinxiang 453000, P. R. China; Corresponding Author Email: fanjl@dlut.edu.cn, zhh1106@htu.edu.cn, Tel/Fax: +86-373-3329030.

Table of Contents

1. Experimental Procedures

Procedures section

The synthesis routes of fluorescent probes **ACx-GGTB** (**AC17-GGTB**, **AC15-GGTB**) and their intermediates are shown in Scheme 1. The reagents used in the synthesis and purification of probes and intermediates were all analytical grade. They were purified by column chromatography using silica gel (200-300 mesh). And the structures were characterized by Avance 600 MHz spectrometer (Bruker Co., Switzerland). Polarimeter (Shanghai Yidian Physical Optical Instrument Co., LTD, China), UV spectrophotometer (GBC Scientific Equipment Pty LTD, Australia) and fluorescence spectrometer (FluoroMax-4, HORIBA, Japan; FS5, Edinburgh Instruments, UK; FLS1000, Edinburgh Instruments, UK) were used for the basic spectral experiments in vitro. And the Biological properties were verified by microplate reader, Liquid Chromatography- Q Exactive Mass Spectrometer (Thermo Fisher, USA), FV1200 spectral confocal multiphoton spectrometer (Olympus, Japan) and polarized optical microscope (Olympus, Japan). Commercial fluorescent dye, ER-Tracker Green, LysoTracker Red DND-99, DiD Perchlorate (DiIC18(5)) was purchased from Beyotime Biotechnology (China). γ-Glutamyltranspeptidase (Enzyme Commission (EC), Number 2.3.2.2) was obtained from Sigma Chemical Co. (USA). 6.0 mM probes solutions (**AC17-GGTB**, **AC15-GGTB**) and control molecules (A, B) were prepared using DMSO for the optical and biological experiments.

Spectrographic determination in vitro.

GGT (0-0.78 U/mL) was added to **AC17-GGTB**, AC17-3 and **AC15-GGTB** (15 μM, PBS, pH = 7.4), respectively. Then the test solution were mixed and left at 37 ^{o}C for 5 min, and the response of the probes to GGT activity was monitored by the changes of UV absorption and fluorescence emission spectral signals. In all spectral experiments, the final solutions contained < 5 ‰ DMSO. All the experimental results were obtained from 5 parallel experiments.

Under the same test conditions above, the fluorescence signal intensity of probe AC17-GGTB (15 μM, PBS, pH = 7.4) at 422 nm under different incubation times (0-4.0 h) was detected to verify the stability of the probe under the test environment.

Rotation measurement.

The probes (**AC17-GGTB**, **AC15-GGTB**) and the metabolites (AC17-3, AC15-3, AC17, AC15, GGTB) were dissolved in dichloromethane (1.5 g/100 mL), and the specific rotation of them were measured with gyroscope at 25 ^{o}C, respectively. The data were obtained from replicate experiments (n = 5).

Photophysical properties determination in vitro.

The photophysical properties of **AC17-GGTB**, AC17 and control molecules A and B were tested in different polar solutions in vitro. The test solution (6.7 μM) was obtained by adding the above four molecules into 9 solvents, including PBS (pH = 7.4), dimethyl sulfoxide, methanol, chloroform, ethyl acetate, tetrahydrofuran, dichloromethane, toluene and n-hexane, respectively. The UV absorption spectra and fluorescence emission spectra were measured using the fluorescence spectrometer FS5 (Edinburgh Instruments, UK) under corresponding excitation and emission wavelengths. The molar extinction coefficient (ε) was calculated using Lambert-Beer law (A = εbC). Additionally, the absolute quantum yields were measured using the ultrafast wide spectrum fluorescence test system (FLS1000, Edinburgh, UK) with assistance from the integrating sphere. The formula for calculating absolute quantum yield with the aid of instrument software is $\emptyset = \frac{N_{em}}{N_{abs}} = \frac{S_{em} - B_{em}}{B_{sc} - S_{sc}}$. Here, N_{em} represents the number of photons emitted, N_{abs} represents the number of photons absorbed, S_{em} represents the number of photons emitted by the sample, B_{em} represents the number of excitation photons scattered by the blank solvent, Ssc represents the number of excitation photons scattered by the sample, and Bsc represents the number of

excitation photons scattered by the blank solvent. In all the spectral experiments, the DMSO content in final solution was less than 5‰. All experimental results were obtained from 5 parallel experiments.

The probe **AC17-GGTB** was continuously added to 3.0 mL of PBS (3.0 mL, pH = 7.4). Then, the fluorescence emission spectrum of **AC17-GGTB** at different concentrations (2-33 μM) were determined using a fluorescence spectrometer FS5 (Edinburgh Instruments, UK). The data were obtained from replicate experiments (n = 5).

The above four molecules (**AC17-GGTB**, AC17, A and B) were added to PBS (pH = 7.4), dimethyl sulfoxide and methanol to obtain the test solution of 6.7 μM. The ultrafast wide spectrum fluorescence test system (FLS1000, Edinburgh, UK) was used to detect the fluorescence lifetime under laser irradiation at 280 nm and 375 nm through the lifetime test mode. The fluorescence lifetime was calculated by fitting the instrument software using the formula $\mathbf{R(t)} = \boldsymbol{B_1 e^{\left(-\frac{t}{\tau 1}\right)}} + \boldsymbol{B_2 e^{\left(-\frac{t}{\tau 2}\right)}} + \boldsymbol{B_3 e^{\left(-\frac{t}{\tau 3}\right)}} + \boldsymbol{B_4 e^{\left(-\frac{t}{\tau 4}\right)}}$. Here, τ_1, τ_2, τ_3, and τ_4 are the fitting lifetimes while B_1, B_2, B_3, and B4 represent their corresponding proportions. The data were obtained from replicate experiments (n = 5).

Theoretical calculation of the the rate constants of the radiative decays and the non-radiative decays.

Firstly, the equilibrium configurations of ground and excited states are optimized by quantization software Gaussian 16, and the transition dipole moments and their derivatives, nonadiabatic coupling vectors, spin-orbit coupling constants, vibrational frequencies and vibrational canonical modes are calculated under the corresponding configuration. After that, MOlecular MAterials Property Prediction Package (MOMAP) software is used to further calculate thermal vibration correlation function of each spectrum and rate, and Fourier transform the thermal vibration correlation function to obtain the radiative and non-radiative transition rates.

Selectivity.

Seven biological macromolecules including bovine serum albumin, amylase, lipase, trypsin, lysozyme, protease K and hemoglobin were selected as interferences. These were added (20 times the equivalent of GGT activity) to the probes (**AC17-GGTB**, **AC15-GGTB** (15 μM)) and enzyme metabolites (AC17-3, AC17, AC15 (15 μM)) test solutions (PBS, pH = 7.4), and the change of fluorescence intensity measured, respectively.

Similarly, the biological coexisting substances cation and anion (include $SnCl_2$, $CdCl_2$, $MnCl_2$, $CoCl_2$, $CuSO_4$, $HgCl_2$, $Zn(NO_3)_2{\cdot}6H_2O$, $FeCl_2{\cdot}7H_2O$, $CaCl_2{\cdot}6H_2O$, $FeCl_3{\cdot}6H_2O$, $Al(NO_3)_3$, $NiCl_2{\cdot}6H_2O$, $MgSO_4$, Li_2CO_3, Na_2CO_3, KH_2PO_4, $AgNO_3$) and amino acid (include Glycyl-DL-phenylalanine, lysine, DL-Threonine, glutamic acid, Cystine, Arginine, Glycyl-L-Tyrosine, d-methionine, Glycine, DL-Leucine, serine, DL-Homocysteine, dithiothreitol, glutamic acid, hypoxanthine, L-aspartic acid, Valine) were added to the test solution (PBS, pH = 7.4) at 20 equivalents to detect the change of fluorescence signal and evaluate the interference ability of GGT monitoring.

Photostability in solution.

The probes (**AC17-GGTB**, **AC15-GGTB** (15 μM)) and enzyme metabolites (AC17-3, AC17, AC15 (15 μM)) were dissolved in PBS (pH = 7.4). The solutions were irradiated by a 500 W iodine-tungsten lamp situated 250 mm away for 4.5 h. An aqueous solution of sodium nitrite (50 g/L) was placed between the samples and the lamp as a light filter (to cut off the light shorter than 400 nm) and as a heat filter. The photostabilities were expressed in terms of ratio fluorescence intensity (%) calculated from the changes of the fluorescence signal intensity at the maximum strength wave before and after irradiative by iodine-tungsten lamp. The fluorescence intensity was determined. The data were obtained from replicate experiments (n = 5).

pH-stability in solution.

The test solutions with different pH (pH = 2-11) were obtained by adjusting strong acid (HCl) and strong base (NaOH). Then the fluorescence intensity of the probes (**AC17-GGTB**, **AC15-GGTB** (15 μM)) and enzyme metabolites (AC17-3, AC17, AC15 (15 μM)) at different pH test solution were measured using a fluorescence spectrometer, respectively. The changes of fluorescence intensity at different pH values were analyzed, in order to determine the influence of different pH values on the detection of probes to GGT activity. The data were obtained from replicate experiments (n = 5).

Solubility in water.

The probes (**AC17-GGTB**, **AC15-GGTB**) and enzyme metabolites (AC17-3, AC17, AC15) were continuously added into H_2O (3.0 mL), respectively. Then the absorbance of the probes at different concentrations were determined by UV spectrophotometer, and the solubility of the probes in H_2O were obtained according to the Lambert Beer's law (A = εbC). The data were obtained from replicate experiments (n = 5).

Cell culture.

HepG2 (cancer cell line) and CHO (normal cell line) were obtained from the Chinese Academy of Medical Sciences. The red-free Dulbecco's Modified Eagle's Medium (DMEM, WelGene) supplemented with penicillin/streptomycin and 10 % fetal bovine serum (FBS; Gibco) were used for culture cells in a CO_2 incubator at 37 ^{o}C. One day before imaging, the cells were seeded into a glass bottomed dish (MatTek, 35 mm dish with 20 mm well) for incubation 24 h in advance at 37 ^{o}C under 5 wt % /vol CO_2. And then, the cells were incubated with a certain concentration of the probes (**AC17-GGTB**, **AC15-GGTB** (20 μM)) at 37 ^{o}C under 5 wt % /vol CO_2, respectively.

Cytotoxicity.

HepG2 cell lines and CHO cell lines were prepared for cell viability studies in 96-well plates (1×10^5 cells per well that were incubated in 100 μL). The cells were incubated for an additional 24 h with probes (**AC17-GGTB**, **AC15-GGTB**) and enzyme metabolites (AC17-3, AC17, AC15) in different concentrations (5.0, 10, 20 μM). Subsequently, 20 μL 5 mg/mL of 3-(4,5-dimethylthiazol-2-yl)-2,5-diphenyltetrazolium bromide (MTT, Sigma Chemical Co. U.S.A.) was added into each well, followed by further incubation for 4 h at 37 ^{o}C. The DMEM was remove and DMSO (150 μL/well) added to dissolve the reddish-blue crystals. Optical density (OD) was determined by a microplate reader (Spectra Max M5, Molecular Devices) at 490 nm. The results from the six individual experiments were averaged. The relative cell viability (100%) was calculated using the following equation:

$$\text{Cell viability}(\%) = (OD_{probe}\text{-}OD_{k\text{-}probe})/(OD_{ctrl}\text{-}OD_{k\text{-}ctrl}) \times 100 \quad (1)$$

The metabolic analysis of probes in cells.

Then cell lysates were extracted to obtain intracellular metabolites. Three cell samples were analyzed by Liquid Chromatography-Q Exactive Mass Spectrometer. The results were obtained from 5 parallel experiments. The detailed experimental steps are as follows:

(1) Three dishes of HepG2 cells were prepared, two of which as the experimental groups were incubated with **AC17-GGTB** (20 μM) for 0.5 h or 4 h at 37 ^{o}C under 5 wt % /vol CO_2, respectively. Another dish of untreated cells served as a control.

(2) Completely suck out the medium, wash them three times with PBS (pH = 7.4) at 4 ^{o}C, add 1.5 mL water, and freeze the sample at -80 ^{o}C.

(3) Removed samples from -80 ^{o}C after 10 min, thaw at 25 ^{o}C, and then freeze at -80 ^{o}C. After repeated freezing and thawing for three times, the cells were scraped on ice with a cell scraper.

(4) Absorb cell lysate. 4.0 mL methanol: acetonitrile (1:1, V/V) solvent mixture was added to the petri dish (two times), and then sucked out successively into cell lysates for mixing.

(5) Vortex for 1 min, sonicate 10 min (4 ^{o}C water bath).

(6) Frozen in liquid nitrogen for 2 min, thawed at 25 ^{o}C, sonicate 10 min (4 ^{o}C water bath). Repeat three times.

(7) Incubate at -20 ^{o}C for 1.0 h (assisted protein precipitation).

(8) Centrifuge the supernatant at 14,000 rpm and 4 ^{o}C for 15 min. Concentrate the supernatant at 4 ^{o}C and freeze dry using a lyophilizer to obtain a white powder.

(9) The peak retention time of **AC17-GGTB** and AC17 were determined by LC-MS/MS analysis with **AC17-GGTB** and AC17 as standard substances.

(10) Then the samples were analyzed by Thermo Fisher Liquid chromatography-Q Exactive Mass Spectrometer. According to the peak retention time of standard substances, the liquid quality signal of **AC17-GGTB** and its metabolites AC17-1a/ AC17-1b, AC17-3 and AC17 in the sample was determined.

(11) Normalized analysis was performed on the mass spectrometry data of the experimental group with reference to TIC, and the change rules of **AC17-GGTB** and its metabolites AC17-1a/ AC17-1b, AC17-3 and AC17 at each time point were explored.

Fluorescence imaging in cells.

Olympus spectral confocal multiphoton microscope (FV1200) with MaiTai femtosecond laser source (Spectra-Physics) was used in cell imaging. The imaging parameters are as follow. Internal PMTs = 16 bit, pixels = 1600 × 1600. Lasers: 800 nm, 405 nm. The scan ranges were ascertained according to fluorescence of probes.

The HepG2 cells were incubated with the probes (**AC17-GGTB**, **AC15-GGTB** (20 μM)) at 37 °C in 5.0 wt %/vol CO_2 for 3 h, then washed with PBS three times and imaged under two-photon excitation at 800 nm and single-photon excitation at 405 nm (scan range = 420-460 nm). The data were obtained from replicate experiments (n = 5).

The HepG2 cells were pretreated with DON (1.0 mM, DMSO) for 1 h, then incubated with the probes (**AC17-GGTB**, **AC15-GGTB** (20 μM)) for 3 h at 37 °C under 5 wt % /vol CO_2, respectively. And then imaged under two-photon excitation at 800 nm to verify the specific response of the probes to endogenous GGT activity in cells (scan range = 420-460 nm). The data were obtained from replicate experiments (n = 5).

HepG2 cells were were incubated with **AC17-GGTB** (20 μM) and enzyme metabolites (AC17-3, AC17, GGTB (20 μM) and PBS (pH = 7.4, control) for 3 h at 37 ℃ under 5 wt % /vol CO_2, respectively. Then washed with PBS (pH = 7.4) for three times and imaged under two-photon excitation at 800 nm (scan range = 420-460 nm). The enzyme metabolite GGTB did not have fluorescence and its imaging results were similar to those of the PBS control group. The data were obtained from replicate experiments (n = 5).

Colocalization imaging.

ER-Tracker Green, LysoTracker Red DND-99, DiD Perchlorate (DiIC18(5)) were used as standard dyes for ER, lysosome and cell membrane, respectively. The cells were incubated with the **AC17-GGTB** (20 μM) for 2.5 h under 5.0 wt % /vol CO_2 at 37 ℃, and then ER-Tracker Green (5.0 μM), LysoTracker Red DND-99 (5.0 μM) and DiD Perchlorate (DiIC18(5)) (5.0 μM) were added and incubated for 0.5 h. After that, they were washed with PBS three times and imaged under excitation at 405 nm, 488 nm, 559 nm and 635 nm. **AC17-GGTB**: excitation wavelength = 405 nm, scan range = 420-460

nm (Blue Channel); ER-Tracker Green: excitation wavelength = 488 nm, scan range = 505-555 nm (Green Channel); LysoTracker Red DND-99: excitation wavelength = 559 nm, scan range = 580-630 nm (Red Channel); DiD Perchlorate (DiIC18(5)): excitation wavelength = 635 nm, scan range = 650-700 nm (Red Channel). The fluorescence imaging was analyzed by colocalization coefficient. The data were obtained from replicate experiments (n = 5).

Partition coefficients.

The logarithms of the water/octanol partition coefficients (log Poct values) of the probes and its metabolites were estimated using the computational procedure of Hansch and Leo. This procedure was used as it permits calculation of the log Poct values, as was required to discuss permeability, and also for use with the QSAR models. Log Poct estimations using the software available at this time do not provide values for ions, but only for the related nonionic bases.

Plane polarization imaging in cells.

In this work, plane polarization imaging was carried out by plane polarization microscope (Olympus, Japan), which is added in the form of attachment to the olympus spectral confocal multiphoton microscope (Olympus, Japan). The plane polarization microscope mainly consists of a light source (DIC illumination), two polarizing devices (polarizer and analyzer) and a detector, which converts the light into linear polarizing through two polarizing devices, and emits optical rotation signals of different intensity under the birefringence characteristics of the sample for polarizing imaging. All polarizing imaging results in this work were obtained under the same instrument test conditions, including the same light source (the same incidence angle) and the same orthogonal condition (the vibration direction of the polarizer and the analyzer are perpendicular to each other).

In the cell plane polarization imaging, the model cells whose GGT was restrained were incubated with AC17-GGTB (20 μM) and enzyme metabolites (AC17-3, AC17, GGTB (20 μM) and PBS (pH = 7.4, control) for 3 h at 37 ℃ under 5 wt % /vol CO_2, respectively. Then washed with PBS (pH = 7.4) for three times and imaged by the simple polarizing microscope. The data were obtained from replicate experiments (n = 5).

Fluorescence or Plane polarization imaging in tissues.

In this work, all animal experiments involved in this study have been approved by the local research ethics review board of the Animal Ethics Committee of the Xinxiang Medical University (Henan, China, ethics statement Reference No. 2015016). And all the mice were used in accordance with institutional ethics committee regulations and guidelines on animal welfare. The mice used were immunodeficient mice (NU/NU, 5 weeks old) purchased from Beijing Weitong Lihua Laboratory Animal Technology Co., LTD. Mice were placed in an independent ventilated cage box system (IVC) and fed with distilled water and SPF diet. The S180 cells (mouse fibrosarcoma cells) were dispersed in 100 μL PBS (pH = 7.2) at a density of 1×10^6 and injected subcutaneously into the right side of mice to establish a tumor mouse model. When the mouse tumor volume grew to about 100 mm^3, the mouse tumor was obtained. Tissue sections with a thickness of 15 μm were obtained by embedding and freezing sections and placed on glass slides for subsequent imaging experiments.

The probe **AC17-GGTB** (20 μM) and PBS (pH = 7.4, control) were added to the tumor tissue area, respectively, to ensure that the whole tissue section was always covered by the solution. They were incubated at 4 ^oC for 10 h, respectively. Then washed with PBS (pH = 7.4) for three times and sealed. And the fluorescence imaging was performed under two-photon excitation at 800 nm (scan range = 420-460 nm). The results were obtained from 5 parallel experiments.

The probes (**AC17-GGTB**, **AC15-GGTB** (20 μM)) and enzyme metabolites (AC17, AC15, GGTB (20 μM) and PBS (pH = 7.4, control) were added to the tissue area, respectively, to ensure that the whole tissue section was always covered by the solution. They were incubated at 4 ^oC for 10 h, respectively. Then washed with PBS (pH = 7.4) for three times and sealed.

And the plane polarization imaging was performed using a simple polarizing microscope. The images were then imitated by the simple polarizing microscope. The results were obtained from 5 parallel experiments.

Fluorescence-plane polarization coupled imaging in cells.

In this work, the fluorescent-plane polarization dual-mode imaging system was used for the cell imaging. The fluorescent-plane polarization dual-mode imaging system is constructed by adding a polarization imaging attachment (plane polarization microscope, Olympus Corporation, Japan) to the multi-photon confocal microscope imager.

HepG2 cells were incubated in the presence of **AC17-GGTB** (20 μM) for different time (10 min, 30 min, 60 min, 90 min, 120 min), and then fluorescence-plane polarization coupled imaging were performed respectively. The excitation source of fluorescence imaging is 800 nm two-photon excitation source. Plane polarization images are obtained at 10 times the lens of a simple polarizing microscope. Data were obtained from repeated experiments (n = 5).

2. The synthesis and structural characterization of probes

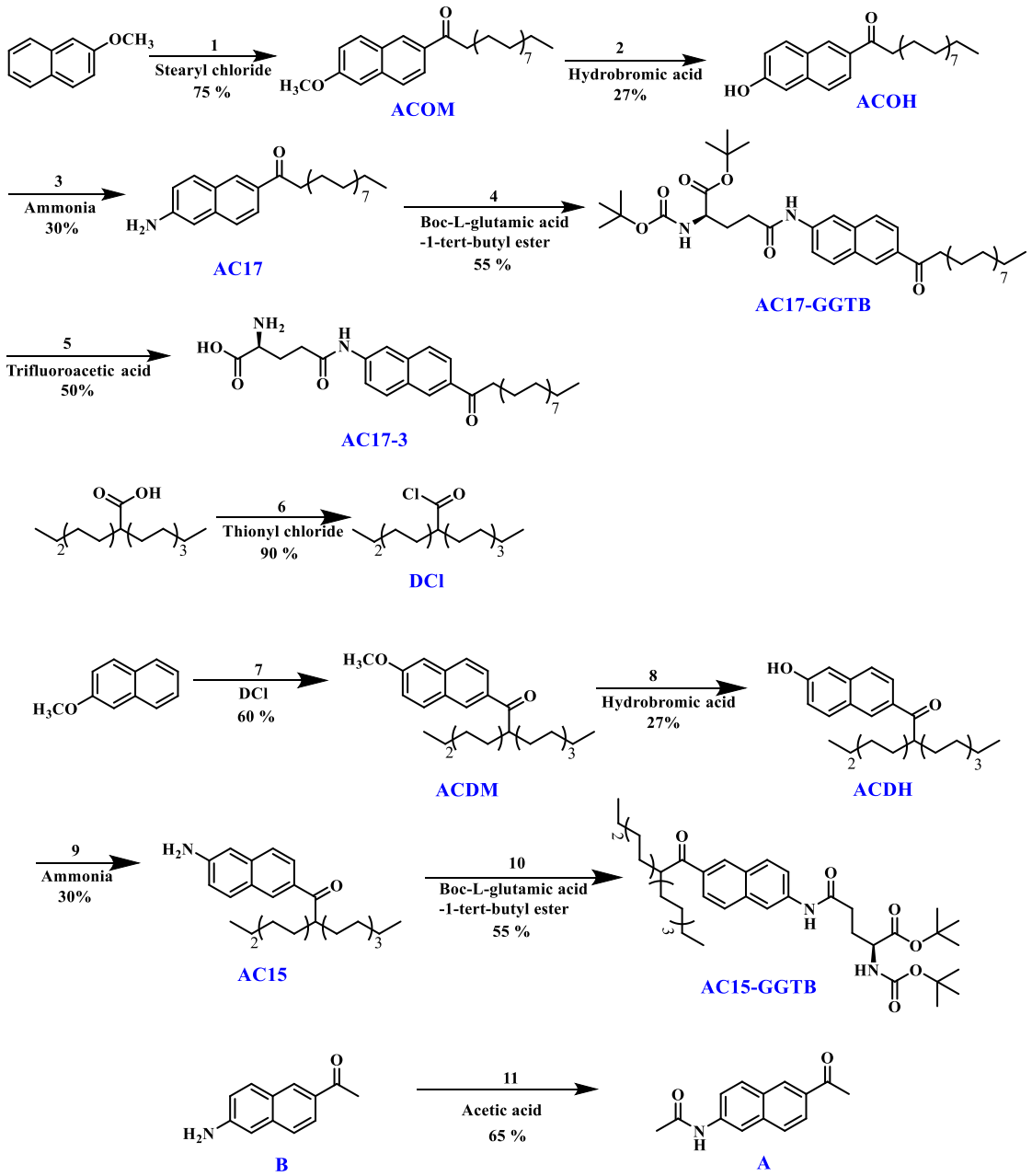

Scheme 1. The synthetic route of **AC17-GGTB**, **AC17-3**, **AC15-GGTB and control molecule A**.

The synthesis of ACOM (1-(6-methoxynaphthalen-2-yl)octadecan-1-one). Under nitrogen protection, anhydrous aluminium trichloride (3.0 mmol, 1.5 eq) and nitrobenzene (1 mL) were added into a two-port round bottom flask with 30 mL anhydrous dichloromethane, and stirred to dissolve. Then cooled to 0 ^{o}C, the 2-Methoxynaphthalene (2.0 mmol, 1.0 eq) was added with stirring to mix, and then stearoyl chloride (2.0 mmol, 1.0 eq) was dropped into the reaction system within 20.0 min. The mixture was stirred at 0 ^{o}C for 6 h and warmed up to 25 ^{o}C for 18 h. The reaction was monitored using TLC. After completion of the reaction, the mixture was poured into 0.1 M ice hydrochloric acid to quench the reaction, and extracted the mixture with dichloromethane. And anhydrous Na_2SO_4 was added, the dichloromethane was removed under reduced pressure and purified by column chromatography using PE/DCM (20:1 to 3:1, v/v) to obtain **ACOM** as a white solid. Yield 75% (0.64 g).^{1}H NMR (600 MHz, $CDCl_3$) δ 8.40 (s, 1H), 8.01 (dd, *J* = 8.6, 1.7 Hz, 1H), 7.85 (d, *J* = 8.9 Hz, 1H), 7.77 (d, *J* = 8.6 Hz, 1H), 7.20 (dd, *J* = 8.9, 2.5 Hz, 1H), 7.16 (d, *J* = 2.3 Hz, 1H), 3.95 (s, 3H), 3.06 (t, *J* = 7.5 Hz, 2H), 1.83 - 1.73 (m, 2H), 1.45 - 1.38 (m, 2H), 1.38 - 1.32 (m, 2H), 1.32 - 1.14 (m, 24H), 0.88 (t, *J* = 7.0 Hz, 3H). ^{13}C NMR (151 MHz, $CDCl_3$) δ 200.28, 159.65, 137.17, 132.54, 131.09, 129.48, 127.88, 127.06, 124.73, 119.64, 105.71, 55.39, 38.55, 31.94, 29.72, 29.69, 29.67, 29.66, 29.56, 29.54, 29.48, 29.38, 24.66, 22.71, 14.13.
HRMS (ESI) Calculated for **ACOM** (M+Na_2+2H) $C_{29}H_{46}O_2Na_2^+$ 472.3150, Found: 472.3178.

The synthesis of ACOH (1-(6-hydroxynaphthalen-2-yl)octadecan-1-one). Compound **ACOM** (1.0 mmol, 1.0 eq) was added to glacial acetic acid (20 mL) and warmed up to 110 ^{o}C, then hydrobromic acid (2.0 mmol, 2.0 eq) was added dropwise and refluxed at 110 ^{o}C for 24 h. The reaction was monitored using TLC. After completion of the reaction, the mixture was cooled to 25 ^{o}C and poured into 200 mL ice water, then adjust the pH to neutral. The mixture was extracted with ethyl acetate and the solvent removed by evaporation under reduced pressure, the crude products were purified by column chromatography using PE/DCM (3:1 to 1:3, v/v) to obtain **ACOH** as a white solid. Yield 27% (0.11 g). ^{1}H NMR (600 MHz, $CDCl_3$) δ 8.41 (s, 1H), 8.00 (dd, *J* = 8.6, 1.7 Hz, 1H), 7.88 (d, *J* = 8.5 Hz, 1H), 7.71 (d, *J* = 8.7 Hz, 1H), 7.20 - 7.14 (m, 2H), 3.11 - 3.01 (m, 2H), 1.83 - 1.75 (m, 2H), 1.45 - 1.38 (m, 2H), 1.38 - 1.32 (m, 2H), 1.29 - 1.24 (m, 24H), 0.88 (t, *J* = 7.0 Hz, 3H). ^{13}C NMR (151 MHz, $CDCl_3$) δ 200.67, 155.72, 137.16, 132.50, 131.71, 129.75, 127.82, 126.74, 124.81, 118.72, 109.57, 38.59, 31.93, 29.71, 29.67, 29.65, 29.54, 29.52, 29.47, 29.37, 24.71, 22.70, 14.13.
HRMS (ESI) Calculated for **ACOH** (M+Li+2H) $C_{28}H_{44}O_2Li^+$ 418.3374, Found: 418.7841.

The synthesis of AC17 (1-(6-aminonaphthalen-2-yl)octadecan-1-one). Compound **ACOH** (1.0 mmol, 1.0 eq) and sodium pyrosulfite (3.0 mmol, 3.0 eq) was mixed with ammonium hydroxide (20 mL) in a pressure reactor and stirred at 140 ^{o}C for 96 h. Then cooled to 25 ^{o}C, the precipitate was filtered and washed with water three times to afford the crude products **AC17**, the crude products were purified by column chromatography using PE/DCM (15:1 to 1:1, v/v) to obtain **AC17** as a white solid. Yield 30% (0.12 g). ^{1}H NMR (600 MHz, $CDCl_3$) δ 8.32 (s, 1H), 7.93 (d, *J* = 8.6 Hz, 1H), 7.76 (d, *J* = 8.4 Hz, 1H), 7.59 (d, *J* = 8.6 Hz, 1H), 6.97 (d, *J* = 10.8 Hz, 2H), 4.06 (s, 2H), 3.03 (t, *J* = 7.3 Hz, 2H), 1.82 - 1.72 (m, 2H), 1.40 (dd, *J* = 14.2, 7.0 Hz, 2H), 1.37 - 1.32 (m, 2H), 1.25 (s, 24H), 0.88 (t, *J* = 6.5 Hz, 3H). ^{13}C NMR (151 MHz, $CDCl_3$) δ 200.31, 146.63, 137.51, 131.33, 131.17, 129.86, 126.57, 125.93, 124.78, 118.67, 107.90, 38.45, 31.94, 29.71, 29.55, 29.51, 29.37, 24.79, 22.70, 14.13.
HRMS (ESI) Calculated for **AC17** (M+CF_3COOH) $C_{30}H_{44}NO_3F_3^-$ 523.3222, Found: 523.2447.

The synthesis of AC17-GGTB (*tert*-butyl N^2-(*tert*-butoxycarbonyl)-N^5-(6-stearoylnaphthalen-2-yl)-*D*-glutaminate). **AC17** (1.5 mmol, 1.0 eq), Boc-Glu-OtBu (1.5 mmol, 1.0 eq), 1-Ethyl-3-(3-dimethylaminopropyl)carbodiimide (2.3 mmol, 1.5 eq), and 4-dimethylaminopyridine (0.75 mmol, 0.5 eq) were dissolved in dichloromethane (20 mL) and stirred at 25 ^{o}C for 24 h. The reaction was monitored using TLC. After completion of the reaction, the dichloromethane was removed by evaporation under reduced pressure, the crude products were purified by column chromatography using PE/DCM (2:1 to

1:10), v/v) to obtain **AC17-GGTB** as a white solid. Yield 55% (0.57 g). ^{1}H NMR (600 MHz, $CDCl_3$) δ 9.37 (s, 1H), 8.40 (s, 2H), 8.00 (d, *J* = 8.6 Hz, 1H), 7.90 (d, *J* = 8.7 Hz, 1H), 7.83 (d, *J* = 8.6 Hz, 1H), 7.64 (d, *J* = 8.4 Hz, 1H), 5.43 (d, *J* = 7.4 Hz, 1H), 4.27 (s, 1H), 3.07 (t, *J* = 7.4 Hz, 2H), 2.52 (t, *J* = 6.0 Hz, 2H), 2.31 (s, 1H), 1.90 (s, 1H), 1.78 (dd, *J* = 14.9, 7.5 Hz, 2H), 1.50 (s, 9H), 1.46 (s, 9H), 1.43 - 1.38 (m, 2H), 1.38 - 1.33 (m, 2H), 1.26 (s, 24H), 0.88 (t, *J* = 6.9 Hz, 3H). ^{13}C NMR (151 MHz, $CDCl_3$) δ 200.45, 171.18, 171.07, 156.84, 138.31, 136.38, 133.42, 130.38, 129.42, 129.27, 128.07, 124.60, 120.56, 115.76, 82.94, 80.73, 53.17, 38.64, 34.39, 31.93, 31.04, 29.70, 29.66, 29.55, 29.54, 29.47, 29.37, 28.35, 27.98, 24.61, 22.70, 14.13.

HRMS (ESI) Calculated for **AC17-GGTB** (M+Li+H) $C_{42}H_{67}N_2O_6Li^+$ 701.5076, Found: 701.4907.

The synthesis of AC17-3 (N^5-(6-stearoylnaphthalen-2-yl)-*L*-glutamine). AC17-GGTB (3.0 mmol, 1.0 eq) was stirred in dichloromethane (20 mL) and trifluoroacetic acid (2 mL) at 25 ^{o}C for 2 h. The reaction was monitored using TLC. After completion of the reaction, the dichloromethane and trifluoroacetic acid were removed by evaporation under reduced pressure to provide the crude product **AC17-3**. The crude products were purified by column chromatography using DCM/MeOH (400:0 to 400:1), v/v) to obtain **AC17-3** as a white solid. Yield 50% (0.81 g). ^{1}H NMR (600 MHz, $CDCl_3$) δ 9.39 (s, 1H), 8.37 (s, 1H), 8.29 (s, 1H), 7.98 (d, *J* = 8.5 Hz, 1H), 7.85 (d, *J* = 8.8 Hz, 1H), 7.78 (d, *J* = 8.6 Hz, 1H), 7.55 (d, *J* = 8.5 Hz, 1H), 3.46 (dd, *J* = 8.4, 4.2 Hz, 1H), 3.05 (t, *J* = 7.4 Hz, 2H), 2.64 (d, *J* = 14.6, 7.3 Hz, 1H), 2.61 - 2.52 (m, 1H), 2.24 (d, *J* = 13.2, 7.3 Hz, 1H), 2.08 (s, 2H), 1.91 (d, *J* = 14.7, 6.7 Hz, 1H), 1.83 - 1.71 (m, 2H), 1.46 (s, 8H), 1.40 (dd, *J* = 14.8, 7.0 Hz, 2H), 1.37 - 1.32 (m, 2H), 1.25 (s, 16H), 0.88 (t, *J* = 6.9 Hz, 3H). ^{13}C NMR (151 MHz, $CDCl_3$) δ 200.48, 174.58, 171.52, 138.24, 136.36, 133.36, 130.37, 129.33, 129.27, 127.97, 124.60, 120.43, 115.64, 81.76, 54.35, 38.64, 34.61, 31.93, 29.87, 29.70, 29.68, 29.66, 29.55, 29.54, 29.46, 29.37, 28.03, 27.96, 24.61, 22.69, 14.13.

HRMS (ESI) Calculated for **AC17-3** (M+Na_2+4H) $C_{33}H_{54}N_2O_4Na_2^+$ 588.3630, Found: 588.4104.

The synthesis of ACDM (2-hexyl-1-(6-methoxynaphthalen-2-yl)decan-1-one). 2-hexyldecanoic acid (1.1 mmol, 1.1 eq) was added to a round-bottom flask with 20 mL sulfoxide chloride and stirred at room temperature for 3 h. Then the sulfoxide chloride was removed under atmospheric pressure to obtain the yellowish liquid product 2-hexyldecanoic acid (DCL). After that, under a nitrogen atmosphere, anhydrous aluminium trichloride (1.5 mmol, 1.5 eq) and nitrobenzene (1 mL) were added into a two-port round bottom flask with 30 mL anhydrous dichloromethane and the mixture was stirred. Then cooled to 0 ^{o}C, 2-Methoxynaphthalene (1.0 mmol, 1.0 eq) was added to the stirred mixture, and then 2-hexyldecanoic acid (DCl, 1.0 mmol, 1.0 eq) was added dropwise into the reaction system within 20 min. The mixture was stirred at 0 ^{o}C for 6 h and warmed up to 25 ^{o}C for 18 h. The reaction was monitored using TLC. After completion of the reaction, the mixture was poured into 0.1 M ice hydrochloric acid to quench the reaction and extracted with dichloromethane. The dichloromethane was removed under reduced pressure and the residue purified by column chromatography using PE/DCM (15:1 to 3:1, v/v) to obtain **ACDM** as a white solid. Yield 60% (0.24 g). ^{1}H NMR (400 MHz, $CDCl_3$) δ 8.39 (s, 1H), 8.02 (d, *J* = 8.6 Hz, 1H), 7.87 (d, *J* = 8.9 Hz, 1H), 7.78 (d, *J* = 8.6 Hz, 1H), 7.20 (dd, *J* = 9.0, 2.1 Hz, 1H), 7.16 (s, 1H), 3.95 (s, 3H), 3.61 - 3.49 (m, 1H), 1.79 (d, *J* = 14.1, 6.9 Hz, 2H), 1.58 - 1.47 (m, 2H), 1.24 (dd, *J* = 15.5, 7.9 Hz, 22H), 0.87 - 0.80 (m, 6H). ^{13}C NMR (151 MHz, $CDCl_3$) δ 204.60, 182.90, 159.70, 137.22, 133.25, 131.21, 129.55, 127.97, 127.17, 125.00, 119.63, 105.70, 55.41, 46.06, 45.61, 32.82, 32.23, 31.89, 31.86, 31.70, 29.92, 29.60, 29.59, 29.45, 29.28, 29.27, 29.26, 27.71, 27.68, 27.40, 27.37.

HRMS (ESI) Calculated for **ACDM** (M+NH_4+H) $C_{27}H_{45}NO_2^+$ 415.3399, Found: 415.7772.

The synthesis of ACDH (2-hexyl-1-(6-hydroxynaphthalen-2-yl)decan-1-one). Compound **ACDM** (1.0 mmol, 1.0 eq) was added to glacial acetic acid (20 mL) and warmed up to 110 ^{o}C, then hydrobromic acid (2.0 mmol, 2.0 eq) was added dropwise and refluxed at 110 ^{o}C for 24 h. The reaction was monitored using TLC. After completion of the reaction, the mixture was cooled to 25 ^{o}C and poured into 200 mL ice water, then the pH was adjusted to neutral. The mixture was extracted with ethyl acetate and removed by evaporation under reduced pressure, the crude products were purified by column

chromatography using PE/DCM (5:1 to 1:2, v/v) to obtain **ACDH** as a white solid. Yield 27% (0.10 g). ^{1}H NMR (400 MHz, DMSO-d_6) δ 10.22 (s, 1H), 8.53 (s, 1H), 7.97 (d, *J* = 8.9 Hz, 1H), 7.87 (dd, *J* = 8.7, 1.5 Hz, 1H), 7.74 (d, *J* = 8.7 Hz, 1H), 7.19 - 7.13 (m, 2H), 3.71 - 3.55 (m, 1H), 1.73 - 1.54 (m, 2H), 1.50 - 1.36 (m, 3H), 1.24 - 1.06 (m, 25H), 0.76 (d, *J* = 6.8, 2.5 Hz, 6H). ^{13}C NMR (151 MHz, $CDCl_3$) δ 206.53, 156.83, 137.60, 132.70, 131.78, 130.28, 127.66, 127.00, 124.76, 119.24, 109.70, 46.22, 32.97, 31.83, 31.67, 29.89, 29.56, 29.42, 29.25, 27.75, 27.72, 22.64, 22.60, 14.10, 14.04.
HRMS (ESI) Calculated for **ACDH** (M+CH_3CN+H) $C_{28}H_{42}NO_2^+$ 424.3210, Found: 424.8975.

The synthesis of AC15 (1-(6-aminonaphthalen-2-yl)-2-hexyldecan-1-one). Compound **ACDH** (1.0 mmol, 1.0 eq) and sodium pyrosulfite (3.0 mmol, 3.0 eq) was mixed with ammonium hydroxide (20 mL) in a pressure reactor and stirred at 140 ^{o}C for 96 h. Then cooled to 25 ^{o}C, the precipitate was filtered and washed with water three times to afford the crude products **AC15**, the crude products were purified by column chromatography using PE/DCM (10:1 to 3:1, v/v) to obtain **AC15** as a white solid. Yield 30% (0.11 g). ^{1}H NMR (600 MHz, $CDCl_3$) δ 8.33 (s, 1H), 7.95 (dd, *J* = 8.7, 1.6 Hz, 1H), 7.77 (d, *J* = 8.4 Hz, 1H), 7.60 (d, *J* = 8.7 Hz, 1H), 7.01 - 6.97 (m, 2H), 4.16 (s, 2H), 3.59 - 3.45 (m, 1H), 1.79 (d, *J* = 14.8, 7.3 Hz, 2H), 1.58 - 1.46 (m, 2H), 1.33 - 1.13 (m, 22H), 0.84 (q, *J* = 7.0 Hz, 6H). ^{13}C NMR (151 MHz, $CDCl_3$) δ 204.46, 146.47, 137.51, 132.08, 131.29, 129.90, 126.70, 126.07, 125.03, 118.69, 108.06, 45.86, 32.87, 31.85, 31.69, 29.92, 29.59, 29.44, 29.27, 27.71, 27.68, 22.65, 22.61, 14.10, 14.07.
HRMS (ESI) Calculated for **AC15** (M+Na+H) $C_{26}H_{40}NONa^+$ 405.2957, Found: 405.2752.

The synthesis of AC15-GGTB (*tert*-butyl N^2-(*tert*-butoxycarbonyl)-N^5-(6-(2-hexyldecanoyl)naphthalen-2-yl)-*L*-glutaminate). **AC15** (1.5 mmol, 1.0 eq), Boc-Glu-OtBu (1.5 mmol, 1.0 eq), 1-Ethyl-3-(3-dimethylaminopropyl)carbodiimide (2.3 mmol, 1.5 eq), and 4-dimethylaminopyridine (0.75 mmol, 0.5 eq) were dissolved in dichloromethane (20 mL) and stirred at 25 ^{o}C for 24 h. The reaction was monitored using TLC. After completion of the reaction, the dichloromethane was removed by evaporation under reduced pressure, the crude products were purified by column chromatography using PE/DCM (2:1 to 1:10) , v/v) to obtain **AC15-GGTB** as a white solid. Yield 55% (0.55 g). ^{1}H NMR (600 MHz, $CDCl_3$) δ 9.43 (s, 1H), 8.40 (s, 2H), 8.01 (d, *J* = 8.5 Hz, 1H), 7.91 (d, *J* = 8.5 Hz, 1H), 7.83 (d, *J* = 8.5 Hz, 1H), 7.67 (d, *J* = 8.0 Hz, 1H), 5.49 (d, *J* = 7.4 Hz, 1H), 4.28 (s, 1H), 3.63 - 3.46 (m, 1H), 2.56 (s, 2H), 2.32 (d, *J* = 4.9 Hz, 1H), 1.96 (s, 1H), 1.80 (d, *J* = 14.5, 7.1 Hz, 2H), 1.54 (dd, *J* = 13.1, 6.5 Hz, 2H), 1.48 (dd, *J* = 19.8, 10.8 Hz, 18H), 1.24 (dd, *J* = 21.5, 13.9 Hz, 22H), 0.84 (dd, *J* = 13.2, 6.8 Hz, 6H). ^{13}C NMR (151 MHz, $CDCl_3$) δ 204.71, 171.23, 156.71, 138.36, 136.38, 134.08, 130.43, 129.48, 129.30, 128.14, 124.79, 120.60, 115.79, 82.80, 80.60, 53.37, 46.14, 34.26, 32.73, 31.82, 31.66, 30.50, 29.88, 29.70, 29.54, 29.41, 29.24, 28.34, 27.97, 27.66, 27.63, 22.62, 22.58, 14.08, 14.04.
HRMS (ESI) Calculated for **AC15-GGTB** (M+Li) $C_{40}H_{62}N_2O_6Li^+$ 672.4753, Found: 672.2648.

The synthesis of control molecule A (*N*-(6-acetylnaphthalen-2-yl)acetamide). Commercialized control molecules B (1-(6-aminonaphthalen-2-yl)ethan-1-one, CAS: 7470-88-4, 0.75 mmol, 1.0 eq), acetic acid (0.75 mmol, 1.0 eq), 1-Ethyl-3-(3-dimethylaminopropyl)carbodiimide (1.2 mmol, 1.5 eq), and 4-dimethylaminopyridine (0.37 mmol, 0.5 eq) were dissolved in dichloromethane (15 mL) and stirred at 25 ^{o}C for 12 h, and the reaction was monitored by TLC. After the reaction was completed, the dichloromethane was removed by vacuum evaporation, and the crude product was purified by PE/DCM (2:1 ~ 1:20, v/v) column chromatography to obtain white solid A. The yield was 65% (0.11 g). ^{1}H NMR (600 MHz, $CDCl_3$) δ 8.40 (s, 1H), 8.25 (s, 1H), 8.01 (dd, *J* = 8.6, 1.5 Hz, 1H), 7.90 (d, *J* = 8.8 Hz, 1H), 7.82 (d, *J* = 8.6 Hz, 1H), 7.53 (d, *J* = 9.0 Hz, 2H), 2.71 (s, 3H), 2.26 (s, 3H). ^{13}C NMR (151 MHz, $CDCl_3$) δ 197.96, 168.58, 137.74, 136.38, 133.70, 130.58, 129.83, 129.50, 128.09, 124.72, 120.43, 115.96, 26.66, 24.85.

3. The specific response of probes to GGT activity in solution

(1) The fluorescence spectra of probes for GGT activity.

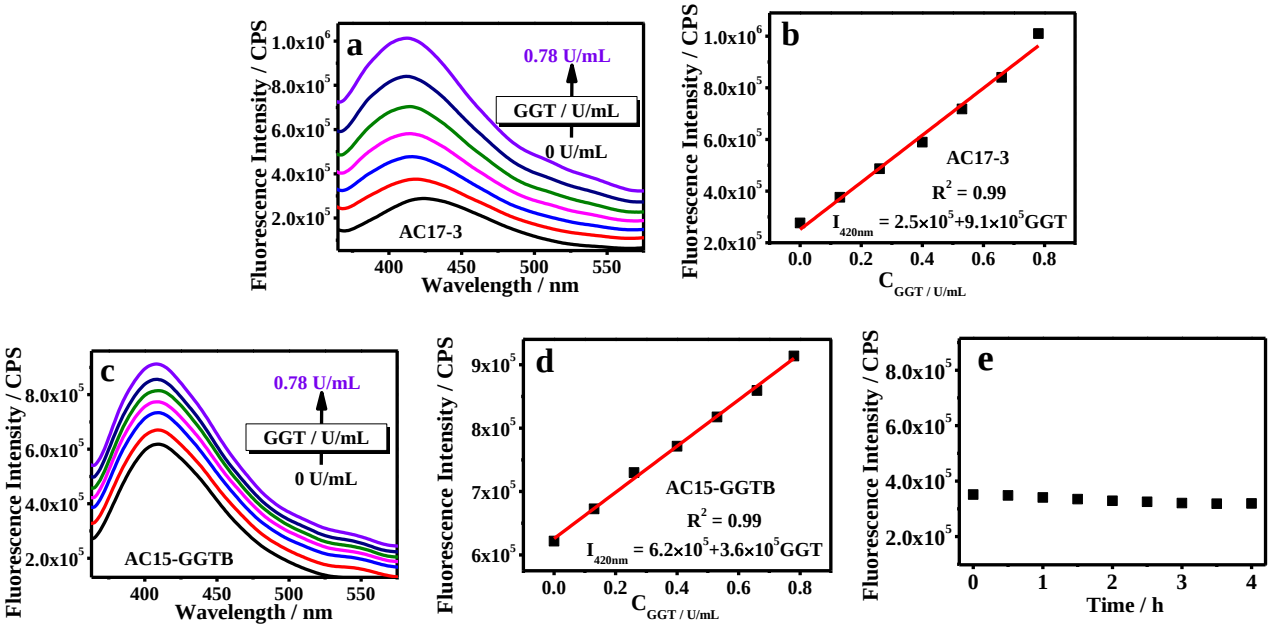

Figure S1. The response of **AC17-3** (15 μM, a, b) and **AC15-GGTB** (15 μM, c, d) towards GGT activity (0-0.78 U/mL) in PBS (pH = 7.4, 37 °C). (a, c), The emission spectrum of probe towards GGT activity (a, **AC17-3**, λ_{ex} = 317 nm; c, **AC15-GGTB**, λ_{ex} = 325 nm). (b, d), The linear response of probe for GGT activity in the emission spectrum (a, c) (b, **AC17-3**, $I_{425\ nm} = 2.5\times10^5+9.1\times10^5$ GGT (R^2 = 0.99); d, **AC15-GGTB**, $I_{410\ nm} = 6.2\times10^5+3.6\times10^5$ GGT (R^2 = 0.99). e, The stability of the AC17-GGTB (15 μM) in PBS (pH = 7.4, 37 °C) for 4.0 h. Data are representative of replicate experiments (n = 5).

(2) The UV absorption spectra of probes for GGT activity.

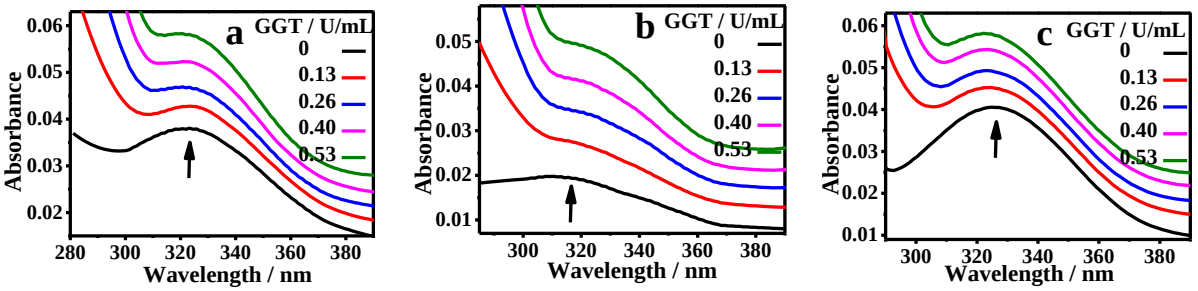

Figure S2. The UV absorption spectra of **AC17-GGTB** (a, 15 μM), **AC17-3** (b, 15 μM) and **AC15-GGTB** (c, 15 μM) for GGT activity in PBS (pH = 7.4, 37 °C). Data are representative of replicate experiments (n = 5).

(3) The selectivity of probes for GGT activity.

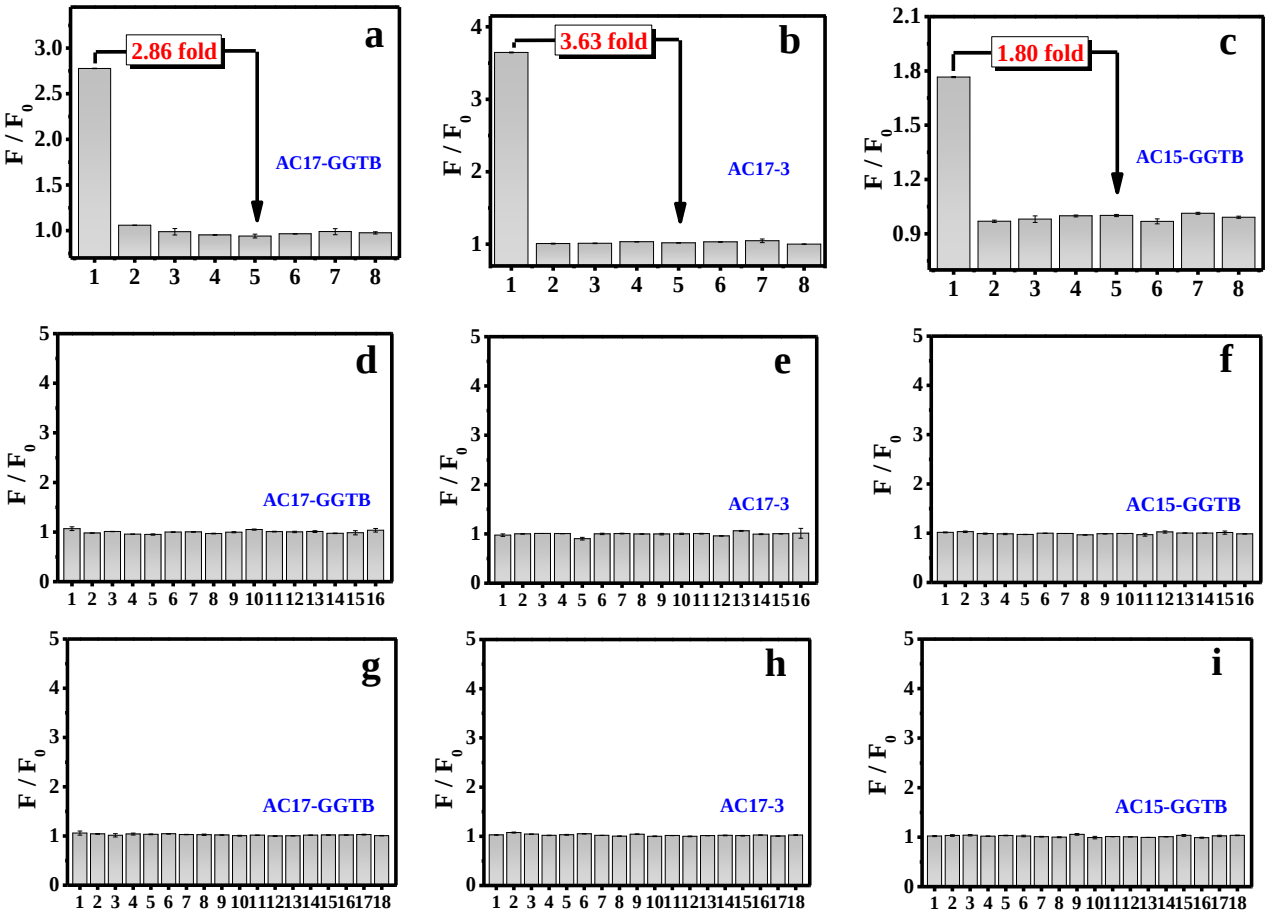

Figure S3. The selectivity of **AC17-GGTB** (15 μM), **AC17-3** (15 μM) and **AC15-GGTB** (15 μM) for GGT activity. (a - c), ion interference results (their concentrations are 20 eq to probes, a, **AC17-GGTB**; b, **AC17-3**; c, **AC15-GGTB**). 1, NaCl; 2, $Pb(NO_3)_2$; 3, Na_2CO_3; 4, $CuSO_4$; 5, $Al(NO_3)_3$; 6, $MaSO_4$; 7, $NiCl_2.6\ H_2O$; 8, Li_2CO_3; 9. KH_2PO_4; 10, K_2HPO_4; 11, $CrCl_3.6\ H_2O$; 12, $ZnSO_4$; 13, $FeCl_3$; 14, $HgCl_2$; 15, $AgNO_3$; 16, $CaCl_2$. (d - f), amino acid interference results (their concentrations are 20 eq to probes, d, **AC17-GGTB**; e, **AC17-3**; f, **AC15-GGTB**). 1, F - DL -phenylalanine; 2, lysine; 3, DL-Threonine; 4, glutamine; 5, cystine; 6, Arginine; 7, F-L-tyrosine; 8, D-methionine; 9, (S)-2-Amino-3-mercaptopropionic acid; 10, glycine; 11, DL-Leucine; 12, serine; 13, DL-Homocysteine; 14, dithiothreitol; 15, glutamic acid; 16, hypoxanthine;17, L-aspartic acid; 18, valine. Data are obtained by the representative of replicate experiments (n = 5).

(4) The HRMS spectrum of AC17-GGTB for GGT activity.

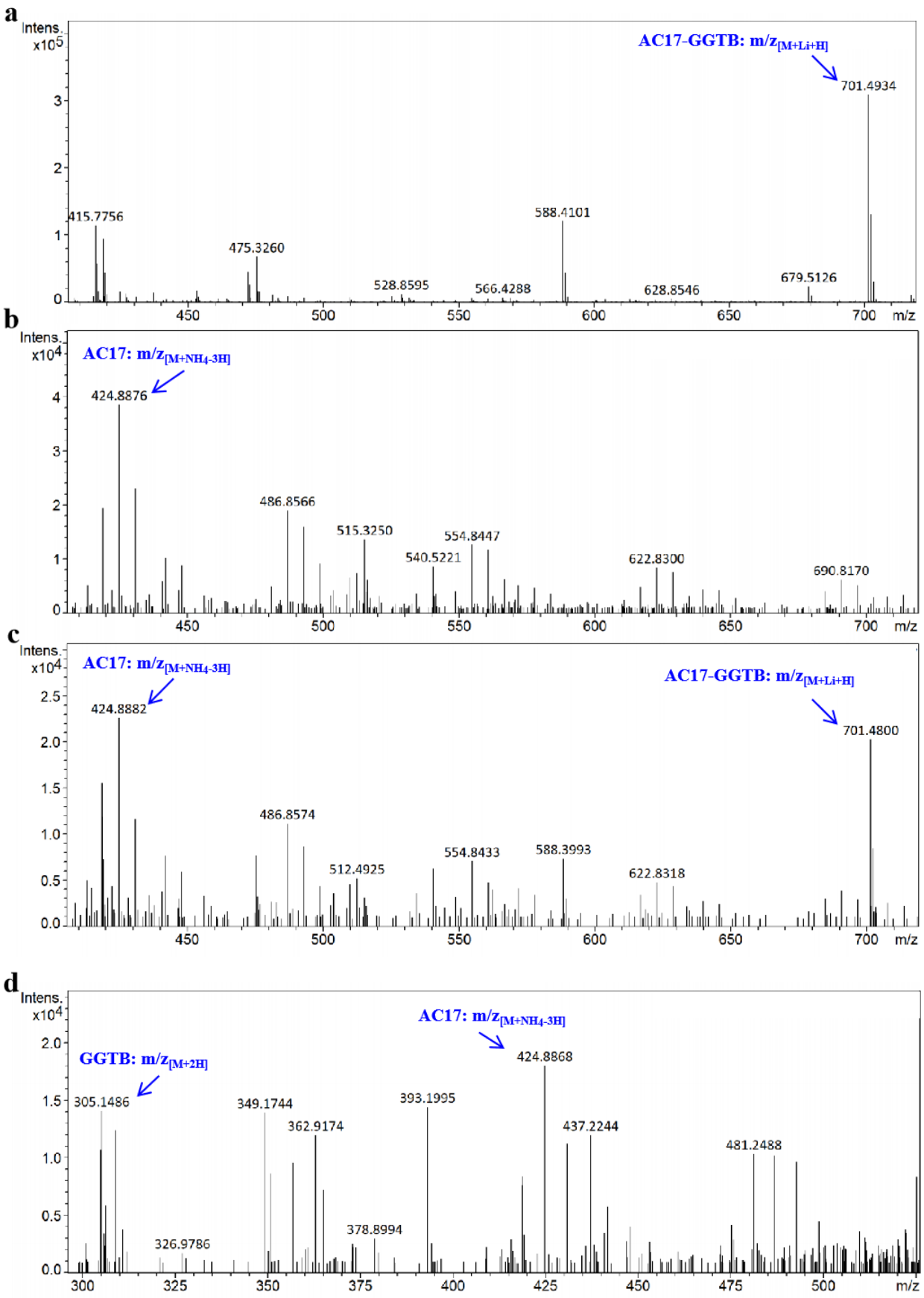

Figure S4. The HRMS spectra of **AC17-GGTB** response to GGT. (a), The HRMS spectra of **AC17-GGTB** before reaction with GGT; (b), The HRMS spectra of metabolite **AC17**; (c, d), The HRMS spectra of **AC17-GGTB** reacting with GGT.

(5) The UV absorption and fluorescence emission spectra of AC17-GGTB, AC17 and commercial molecules A and B.

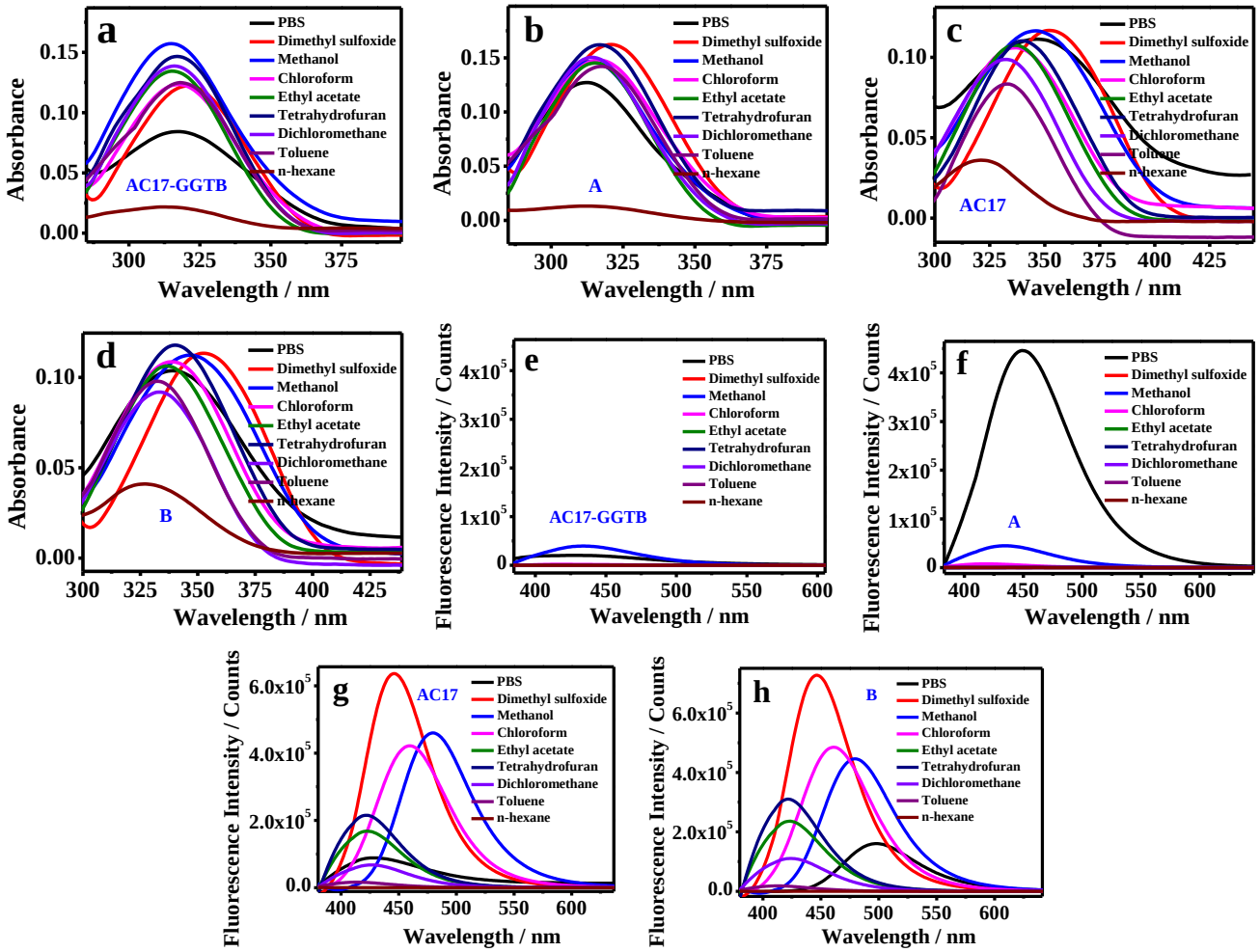

Figure S5. The UV absorption (a-d) and fluorescence emission spectra (e-h) of **AC17-GGTB** (a, e, 6.7 μM), commercial molecules A (b, f, 6.7 μM), AC17 (c, g, 6.7 μM) and commercial molecules B (d, h, 6.7 μM). Data are representative of replicate experiments (n = 5).

(6) The fluorescence lifetimes of AC17-GGTB, AC17 and commercial molecules A and B.

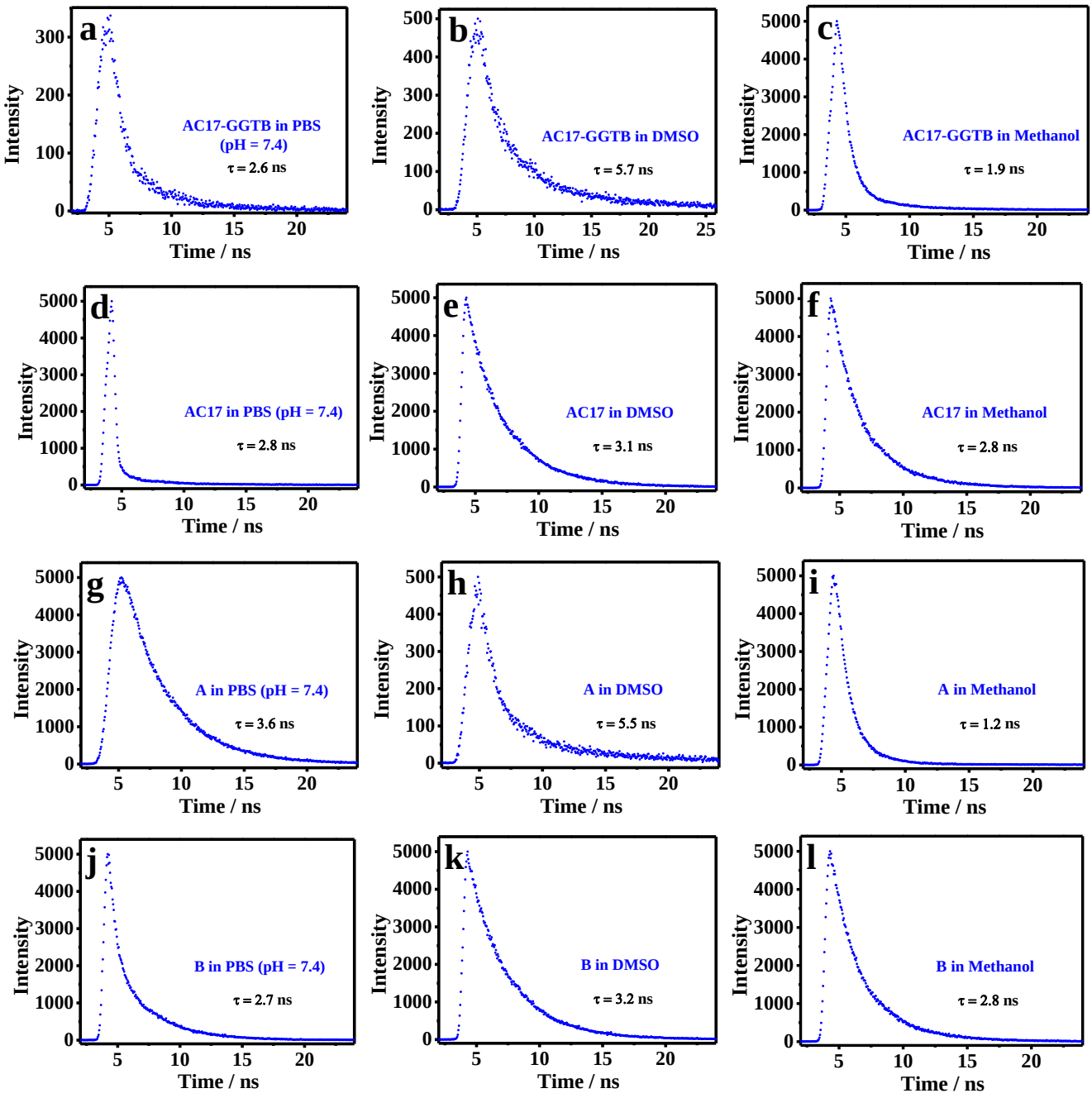

Figure S6. The fluorescence lifetimes of **AC17-GGTB** (a-c, 6.7 μM), commercial molecules A (d-f, 6.7 μM), AC17 (g-i, 6.7 μM) and commercial molecules B (j-l, 6.7 μM).

(7) The photophysical properties in different solvents.

Table S1. Photophysical properties of AC17-GGTB, AC17 and commercial molecules A and B.

		PBS	Dimethyl sulfoxide	Methanol	Chloroform	Ethyl acetate	Tetrahydrofuran	Dichloromethane	Toluene	n-hexane
AC17-GGTB	λ_{ex} / nm	318	320	315	318	316	317	316	318	314
	λ_{em} / nm	422	412	434	417	425	-	424	-	-
	ε / L·mol^{-1}·cm^{-1}	1.3×10^{5}	1.7×10^{5}	2.4×10^{5}	1.9×10^{5}	2.1×10^{5}	2.3×10^{5}	2.1×10^{5}	1.9×10^{5}	3.4×10^{4}
	Φ	0.07	0.0029	0.081	0.0045	0.0018	-	0.0015	-	-
	τ / ns	2.6	5.7	1.9	-	-	-	-	-	-
	K_r / ns^{-1}	2.7×10^{-2}	5.0×10^{-4}	4.3×10^{-2}	-	-	-	-	-	-
	K_{nr} / ns^{-1}	3.6×10^{-1}	1.7×10^{-1}	4.9×10^{-1}	-	-	-	-	-	-
	Radiative decay rate constant (calculated) / ns^{-1}							1.1×10^{-4}		
	Non-radiative decay rate constant (calculated) / ns^{-1}							1.7×10^{2}		
A	λ_{ex} / nm	312	321	314	316	315	317	314	316	313
	λ_{em} / nm	450	412	434	417	428	-	444	-	-
	ε / L·mol^{-1}·cm^{-1}	1.9×10^{5}	2.5×10^{5}	2.2×10^{5}	2.3×10^{5}	2.2×10^{5}	2.5×10^{5}	2.3×10^{5}	2.2×10^{5}	2.1×10^{4}
	Φ	0.013	0.0025	0.043	0.0055	0.0013	-	0.0012	-	-
	τ / ns	3.6	5.5	1.2	-	-	-	-	-	-
	K_r / ns^{-1}	3.6×10^{-3}	4.6×10^{-4}	3.7×10^{-2}	-	-	-	-	-	-
	K_{nr} / ns^{-1}	2.7×10^{-1}	1.8×10^{-1}	8.3×10^{-1}	-	-	-	-	-	-
AC17	λ_{ex} / nm	345	353	346	336	336	340	332	333	323
	λ_{em} / nm	430	445	479	458	422	422	427	413	-
	ε / L·mol^{-1}·cm^{-1}	1.7×10^{5}	1.8×10^{5}	1.8×10^{5}	1.6×10^{5}	1.6×10^{5}	1.7×10^{5}	1.5×10^{5}	1.3×10^{5}	5.6×10^{4}
	Φ	0.21	0.85	0.61	0.53	0.19	0.19	0.056	0.026	0.024

	τ / ns	2.8	3.1	2.8	-	-	-	-	-	-
	K_r / ns^{-1}	7.6×10^{-2}	2.7×10^{-1}	2.2×10^{-1}	-	-	-	-	-	-
	K_{nr} / ns^{-1}	2.6×10^{-1}	4.8×10^{-2}	1.4×10^{-1}	-	-	-	-	-	-
	Radiative decay rate constant (calculated) / ns^{-1}						3.8×10^{-2}			
	Non-radiative decay rate constant (calculated) / ns^{-1}						8.4 ns^{-1}			
	λ_{ex} / nm	340	353	347	339	336	340	333	333	325
	λ_{em} / nm	497	446	480	460	422	421	425	412	-
	ε / L mol^{-1}·cm^{-1}	1.6×10^{5}	1.7×10^{5}	1.7×10^{5}	1.6×10^{5}	1.6×10^{5}	1.8×10^{5}	1.4×10^{5}	1.5×10^{5}	5.0×10^{4}
B	Φ	0.24	0.89	0.57	0.60	0.28	0.25	0.069	0.030	-
	τ / ns	2.7	3.2	2.8	-	-	-	-	-	-
	K_r / ns^{-1}	8.6×10^{-2}	2.7×10^{-1}	2.0×10^{-1}	-	-	-	-	-	-
	K_{nr} / ns^{-1}	2.8×10^{-1}	3.4×10^{-2}	1.5×10^{-1}	-	-	-	-	-	-

Note: The calculation results are based on the calculation of individual molecules, and the related solvent is not added；”-“ is no data.

(8) The fluorescence emission spectra of AC17-GGTB at different concentrations in PBS .

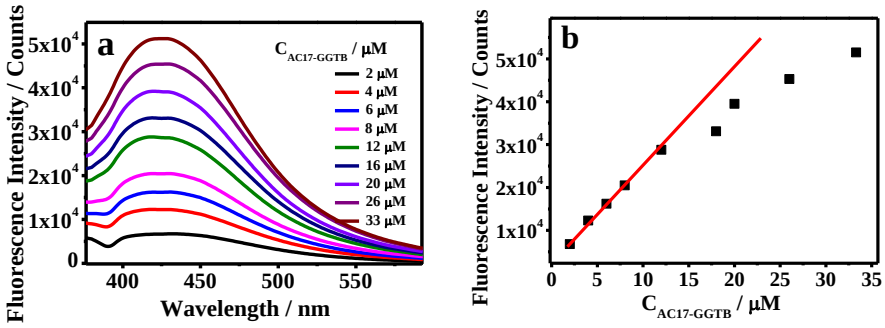

Figure S7. The fluorescence emission spectra (a) of AC17-GGTB at different concentrations in PBS (pH = 7.4). (b) Linear relationship between fluorescence signal intensity (422 nm) and its concentration. Data are representative of replicate experiments (n = 5).

(9) The dynamic response of probes for GGT activity.

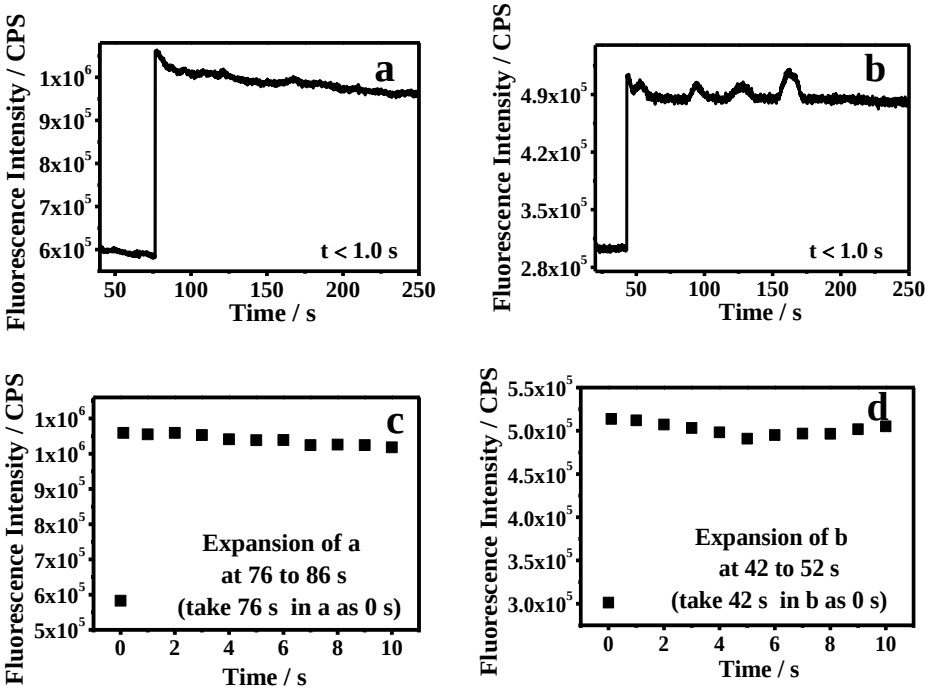

Figure S8. The dynamic response of **AC17-3** (a and c, 15 μM, λ_{ex} = 317 nm) and **AC15-GGTB** (b and d, 15 μM, λ_{ex} = 325 nm) toward GGT activity in PBS (pH = 7.4, 37 ^{o}C). (c, d) The local expansion in (a, take 76 s in (a) as 0 s) or (b, take 42 s in (b) as 0 s).Data are representative of replicate experiments (n = 5).

4. The biocompatibility of probes

(1) The photostability of the probes and the metabolites.

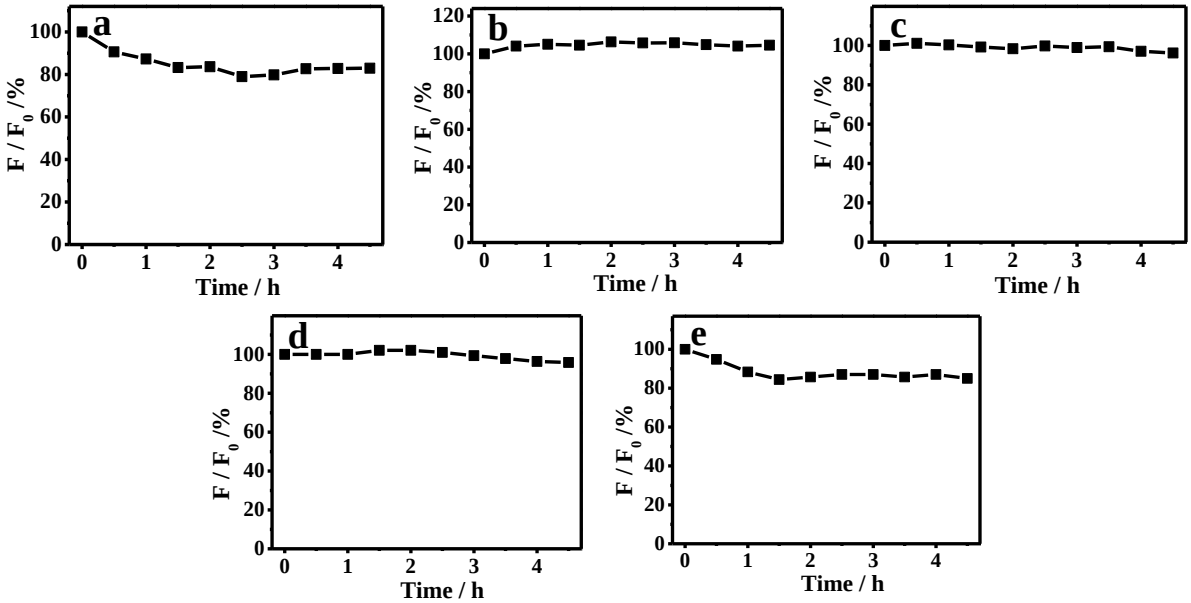

Figure S9. The photostability of **AC17-GGTB** (a), **AC17-3** (b), **AC15-GGTB** (c), **AC17** (d) and **AC15** (e). irradiation time: 4.5 h.

(2) The pH-stability of the probes and the metabolites.

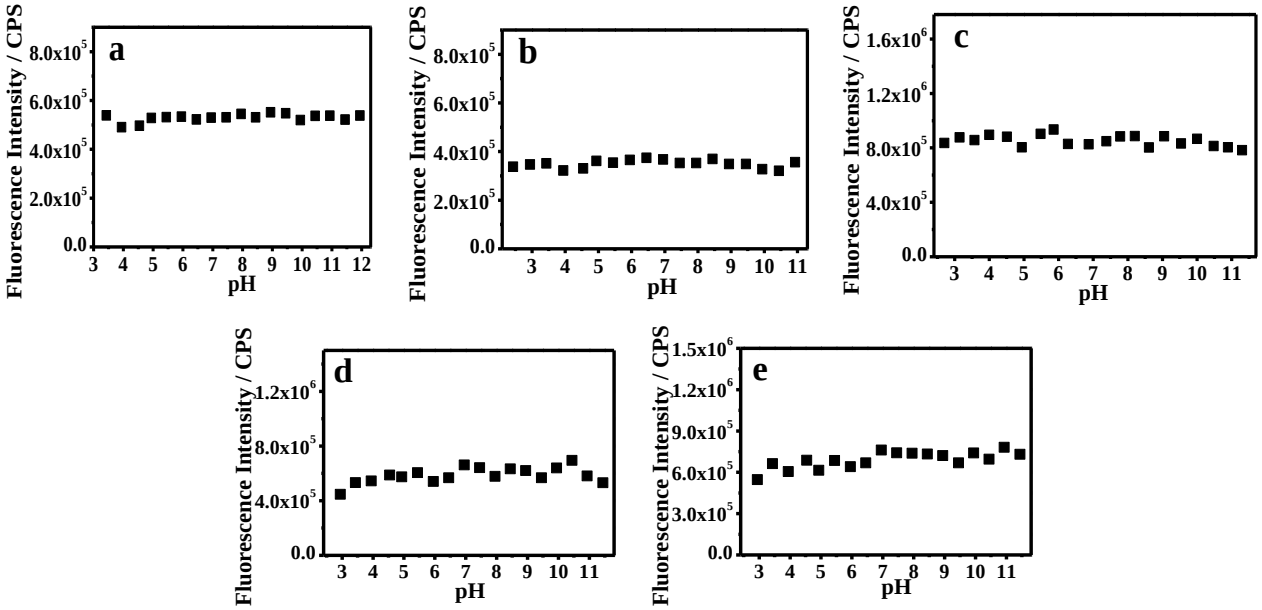

Figure S10. The pH-stability of **AC17-GGTB** (a), **AC17-3** (b), **AC15-GGTB** (c), **AC17** (d) and **AC15** (e).

(3) The water solubility of the probes and the metabolites.

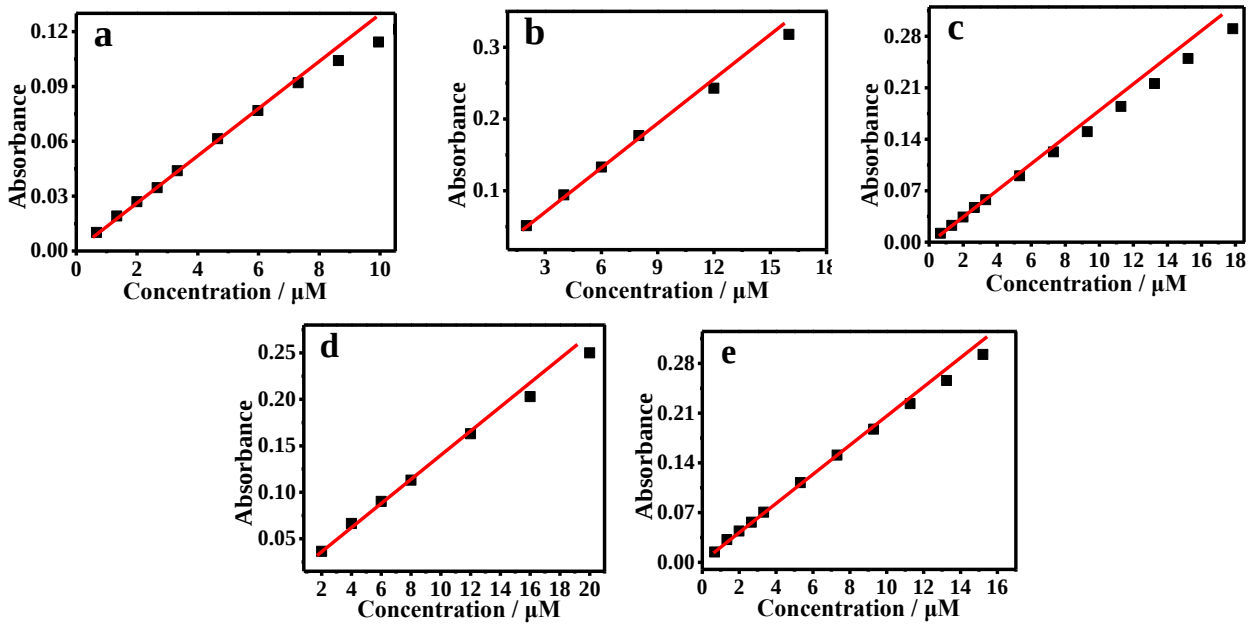

Figure S11. Water solubility of **AC17-GGTB** (a), **AC17-3** (b), **AC15-GGTB** (c), **AC17** (d) and **AC15** (e).

(4) The cytotoxicity of the probes and the metabolites.

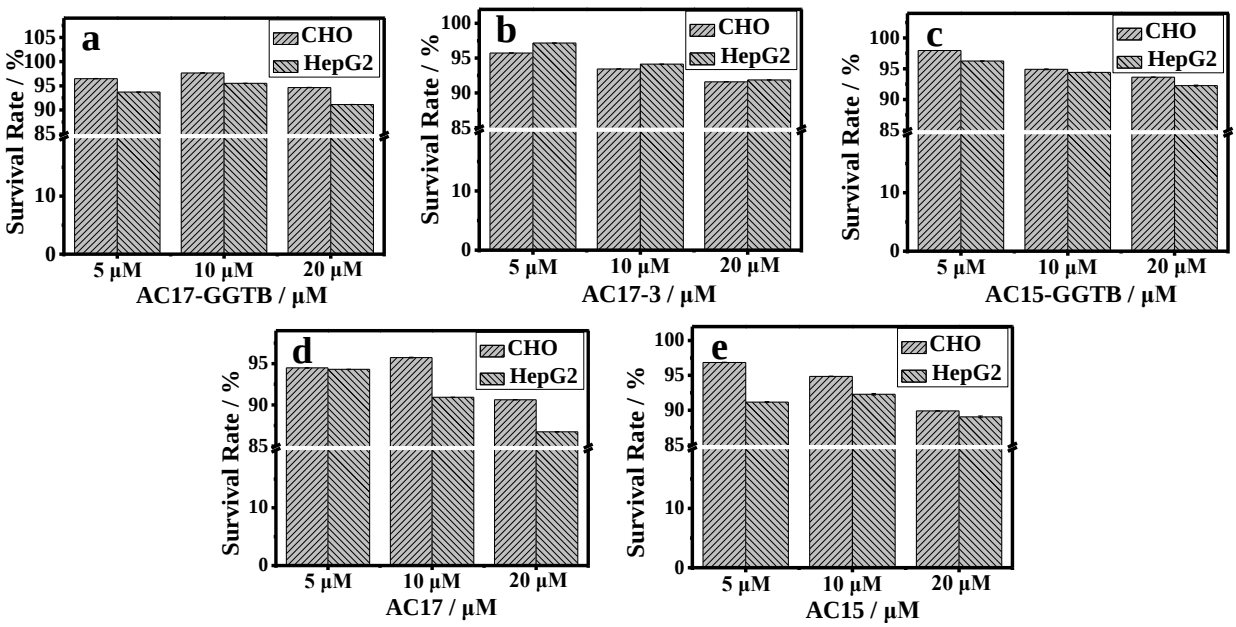

Figure S12. Cytotoxicity toxicity of **AC17-GGTB** (a), **AC17-3** (b), **AC15-GGTB** (c), **AC17** (d) and **AC15** (e).

5. The structural changes of AC17-GGTB in cells

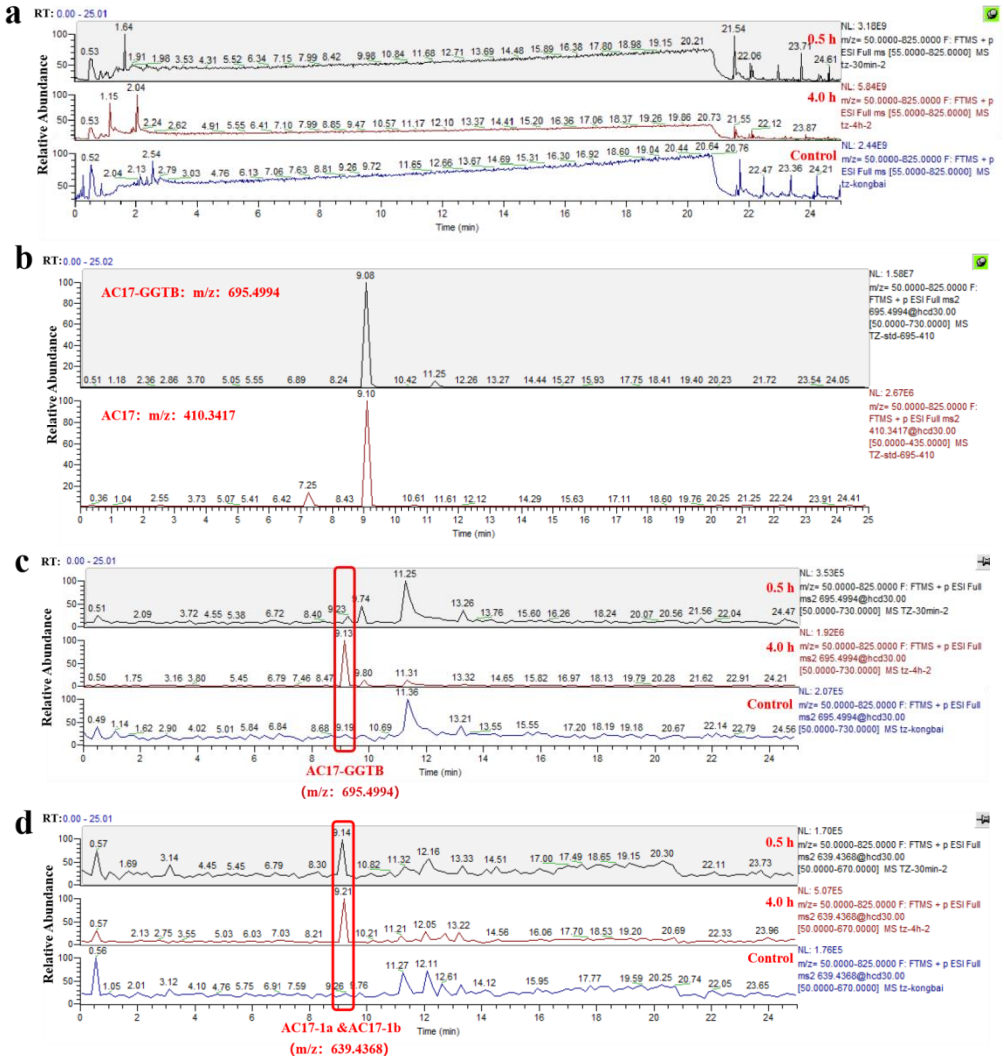

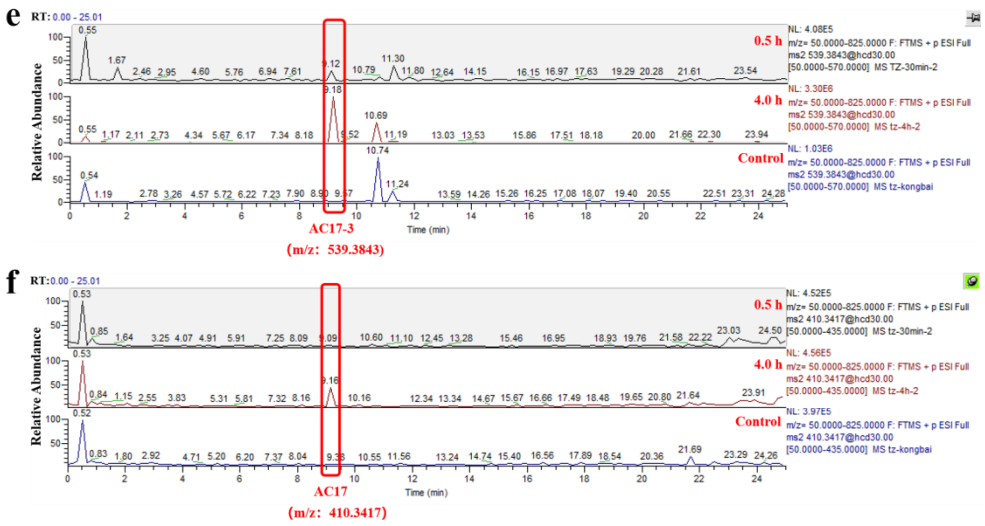

Figure S13. Total ion flow diagram (TIC) of **AC17-GGTB** (20 μM) in cells. (a), the total ion flow diagram (TIC) of the three cell samples; (b), the liquid - mass spectrometry data of **AC17-GGTB** and **AC17**; (c -e), the mass spectra peaks of **AC17-GGTB** (c) and **AC17-1a** and **AC17-1b** (d) and **AC17-3** (e) and **AC17** (f) in liquid-mass spectrometry experiments for three cell samples. The three cell samples included two experimental groups, incubated with **AC17-GGTB** (20 μM) for 0.5 h and 4.0 h, respectively, and a control group without **AC17-GGTB**.

6. The fluorescent or plane polarization imaging of probes for GGT activity

(1) The fluorescence imaging of AC17-GGTB and the enzyme metabolites in cells.

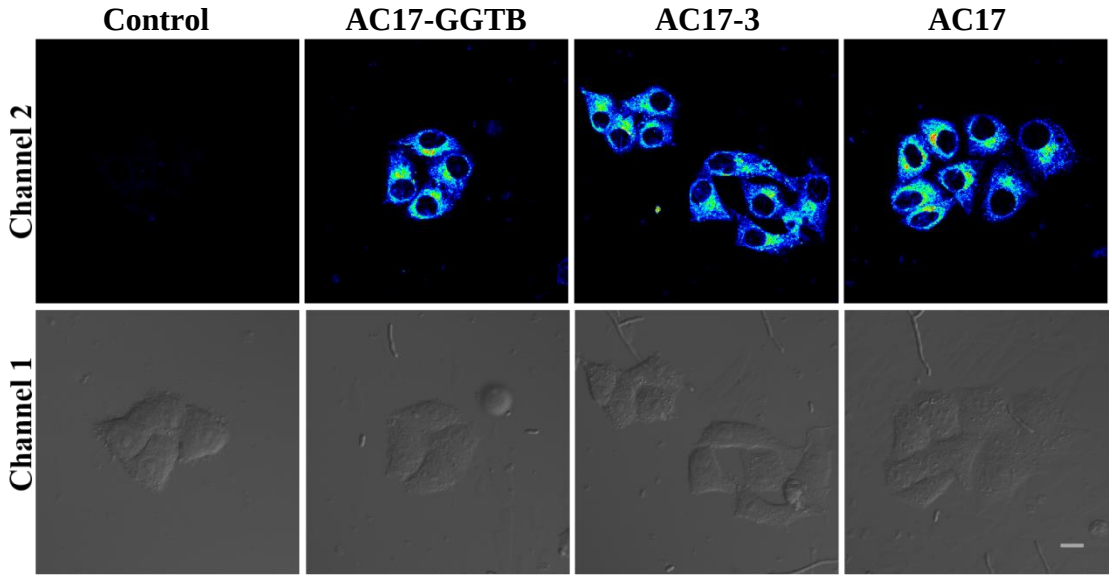

Figure S14. Fluorescence imaging of **AC17-GGTB** and the enzyme metabolites (**AC17-3**, **AC17**) and PBS (pH = 7.4, control) in HepG2 cells. Channel 1: bright channel; Channel 2: fluorescent channel (Two-photon excitation wavelength = 800 nm, scan range = 420-460 nm). Incubation concentration: 20 μM. Incubation time: 3 h. Scan: 10 μm.

(2) The fluorescence imaging of AC17-GGTB for GGT activity in tissues.

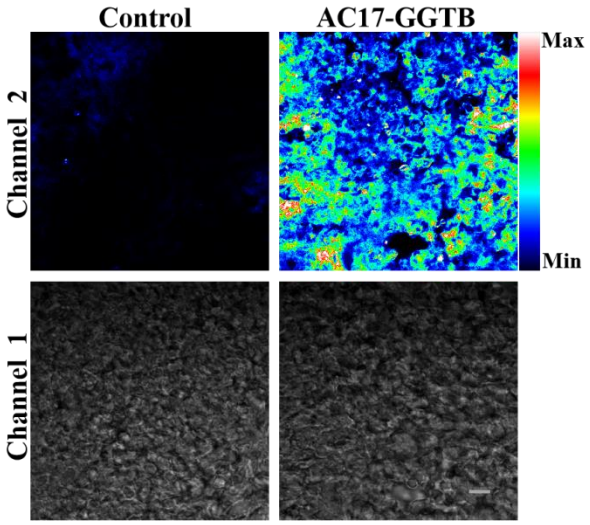

Figure S15. The fluorescence imaging of **AC17-GGTB** for GGT activity in tissues. **AC17-GGTB** showed significantly enhanced fluorescence signal after responding to GGT in tissue. That is, **AC17-GGTB** can be used for highly sensitive fluorescence imaging of GGT in tissues. Channel 1: bright channel; Channel 2: fluorescent channel (Two-photon excitation wavelength = 800 nm, scan range = 420-460 nm). Incubation concentration: 20 μM. Incubation time: 3 h. Scan: 20 mm.

(3) The plane polarization imaging of AC17-GGTB for GGT activity in tissues.

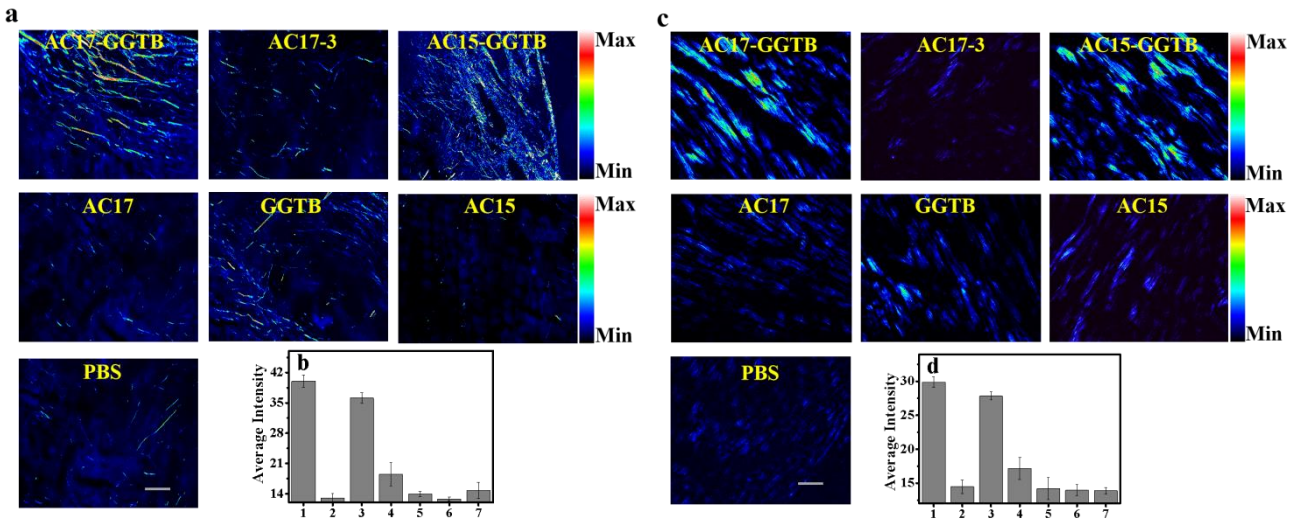

Figure S16. The plane polarization imaging of probes (20 μM) for GGT activity in tissues. (a, c), The plane polarization imaging of probes for GGT activity in mouse tumor tissues (a) and mouse heart tissues (c). (b, d), The optical rotation signal intensity data statistics in (a) or (c). According to the different chiral conformation of **ACx-GGTB** and its metabolites, it presents significantly different optical rotation signals in tissues. So, based on the changes of chiral conformation before and after recognition by GGT in different tissues from mice, **ACx-GGTB** can monitor the GGT activity in tissues by plane polarization imaging. 1, **AC17-GGTB**; 2, **AC17-3**; 3, **AC15-GGTB**; 4, **GGTB**; 5, **AC17**; 6, **AC15**; 7, PBS (pH = 7.4). Section thickness: 15 nm. Incubation concentration: 45 μM. Incubation time: 10 h. Scan: 50 mm.

7. HRMS spectrum

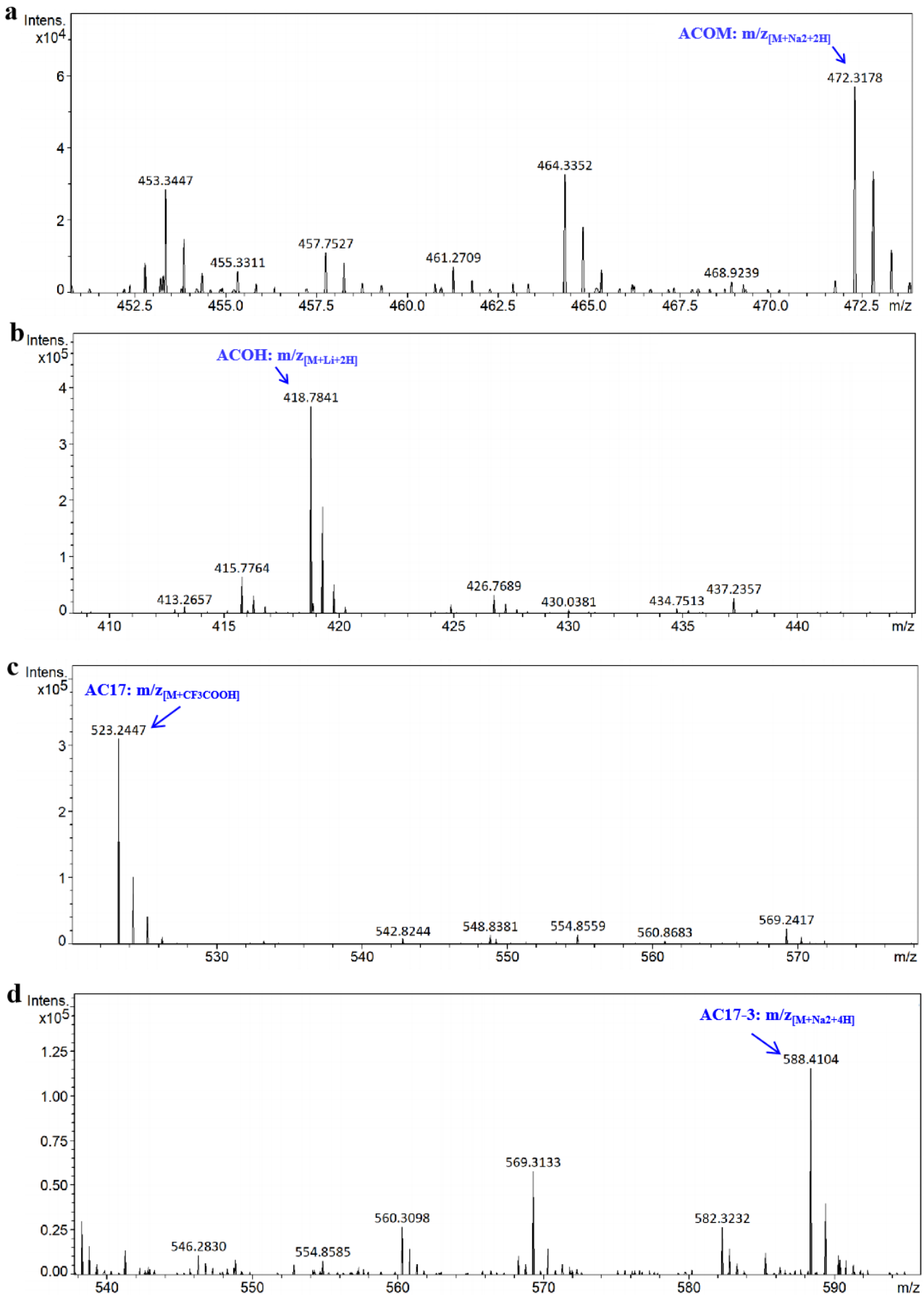

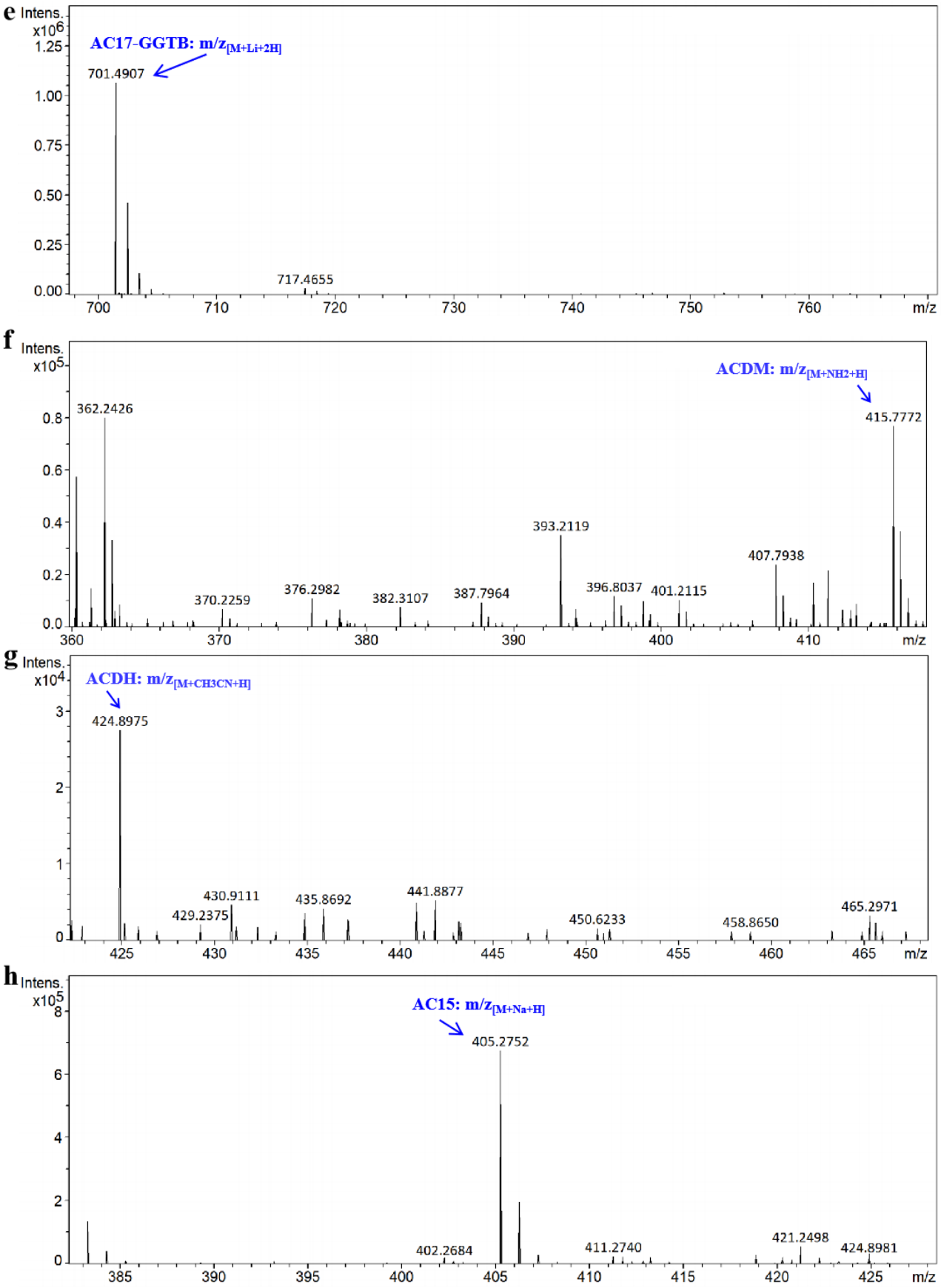
e
Intens.
x10^6
1.25
1.00
0.75
0.50
0.25
0.00
AC17-GGTB: m/z[M+Li+2H]
701.4907
717.4655
700
710
720
730
740
750
760
m/z
f
Intens.
x10^5
0.8
0.6
0.4
0.2
0.0
ACDM: m/z[M+NH2+H]
362.2426
415.7772
393.2119
407.7938
370.2259
376.2982
382.3107
387.7964
396.8037
401.2115
360
370
380
390
400
410
m/z
g
Intens.
x10^4
3
2
1
0
ACDH: m/z[M+CH3CN+H]
424.8975
430.9111
429.2375
435.8692
441.8877
450.6233
458.8650
465.2971
425
430
435
440
445
450
455
460
465
m/z
h
Intens.
x10^5
8
6
4
2
0
AC15: m/z[M+Na+H]
405.2752
402.2684
411.2740
421.2498
424.8981
385
390
395
400
405
410
415
420
425
m/z

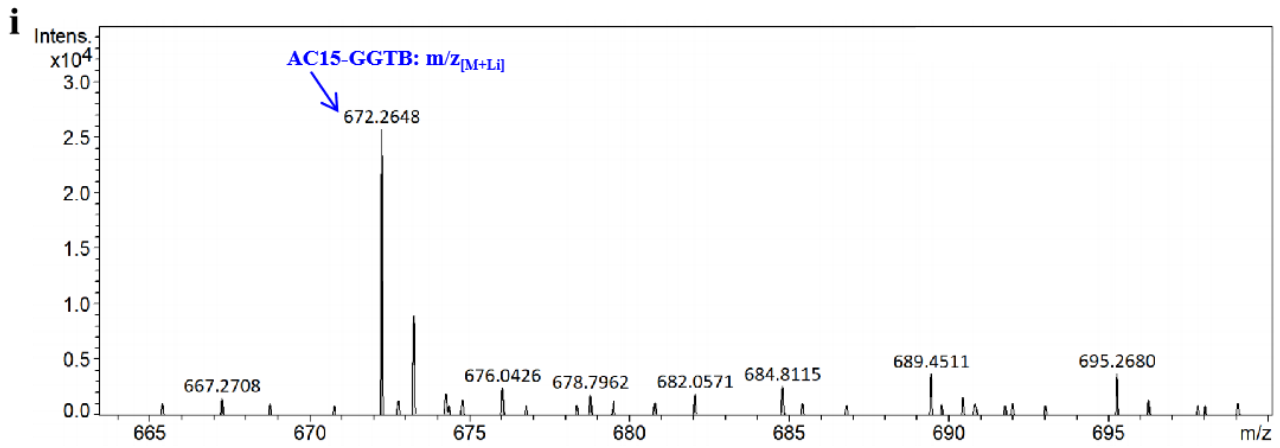

Figure S17. The HRMS spectra of the intermediates (a, **ACOM**; b, **ACOH**; c, **AC17**; d, **AC17-3**; f, **ACDM**; g, **ACDH**; h, **AC15**;) and probes (e, **AC17-GGTB**; i, **AC15-GGTB**).

8 Appendix

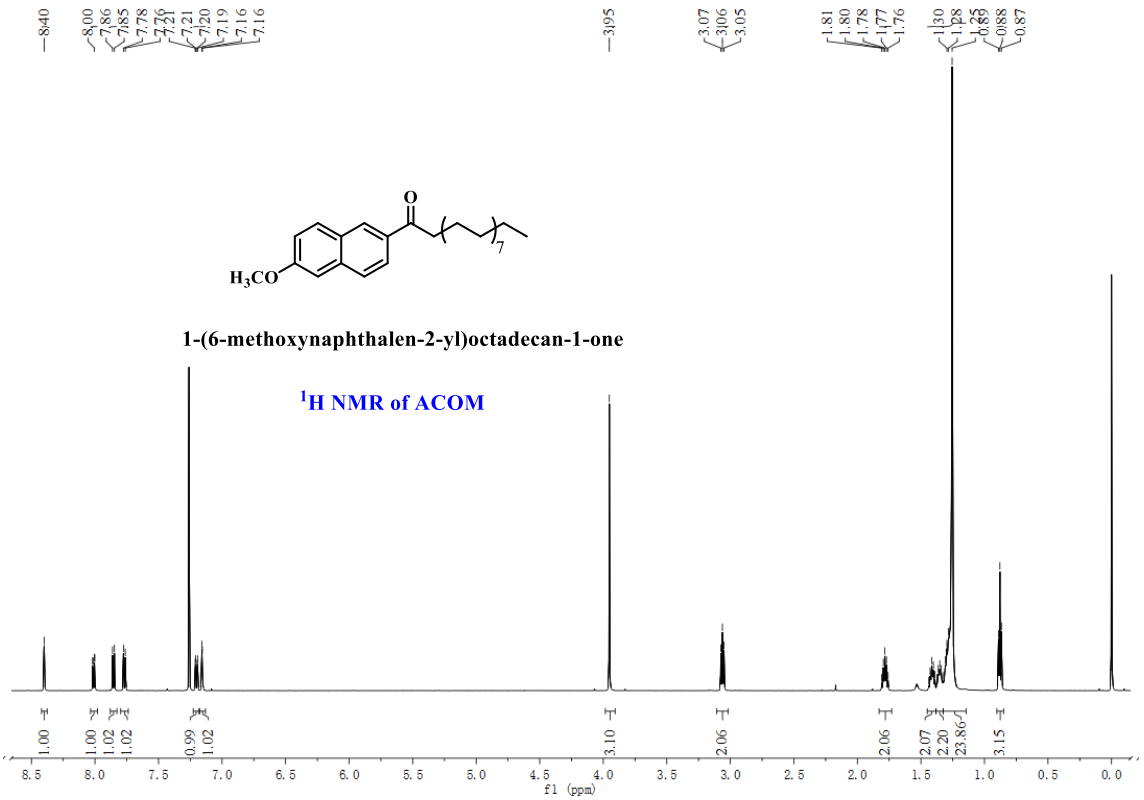
8.40
8.00
7.86
7.85
7.78
7.21
7.20
7.19
7.16
7.16
3.95
3.07
3.06
3.05
1.81
1.80
1.78
1.77
1.76
1.30
1.28
0.89
0.88
0.87
O
H3CO
7
1-(6-methoxynaphthalen-2-yl)octadecan-1-one
1H NMR of ACOM
1.00
1.00
1.02
1.02
0.99
1.02
3.10
2.06
2.06
2.07
2.20
23.86
3.15
f1 (ppm)

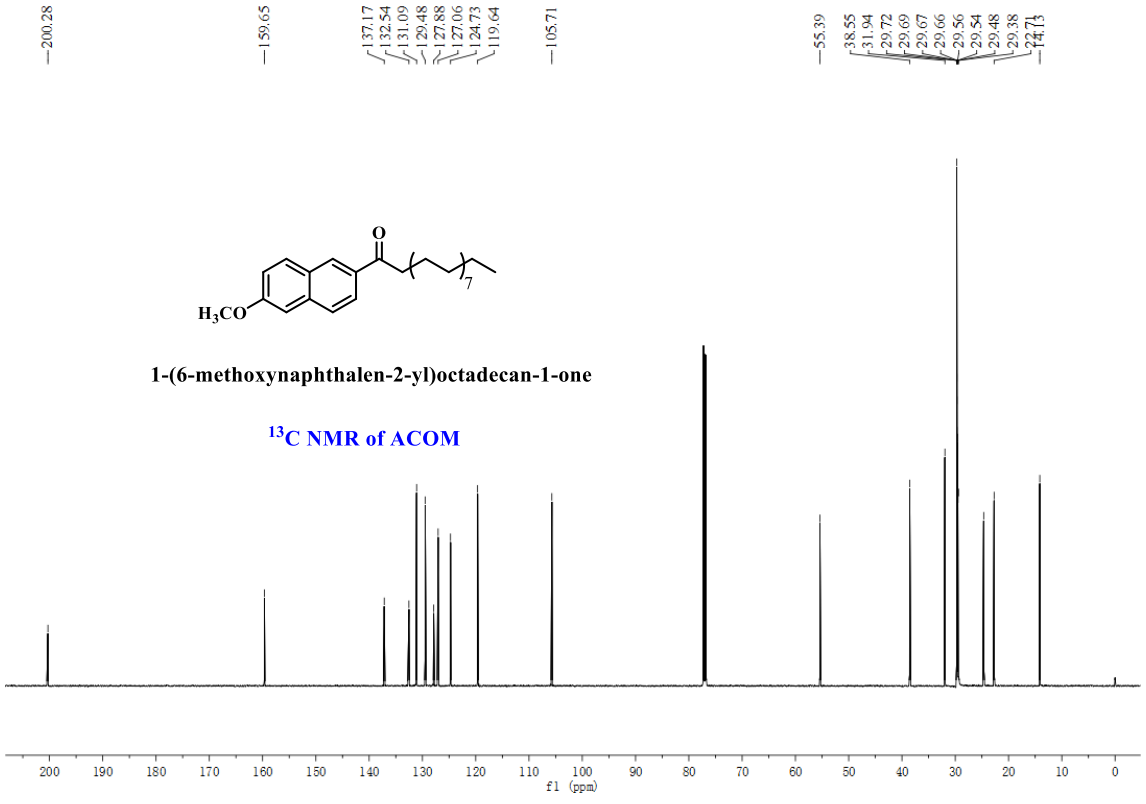
200.28
159.65
137.17
132.54
131.09
129.48
127.88
127.06
124.73
119.64
105.71
55.39
38.55
31.94
29.72
29.69
29.67
29.66
29.56
29.54
29.48
29.38
22.71
14.13
O
H3CO
7
1-(6-methoxynaphthalen-2-yl)octadecan-1-one
13C NMR of ACOM
f1 (ppm)

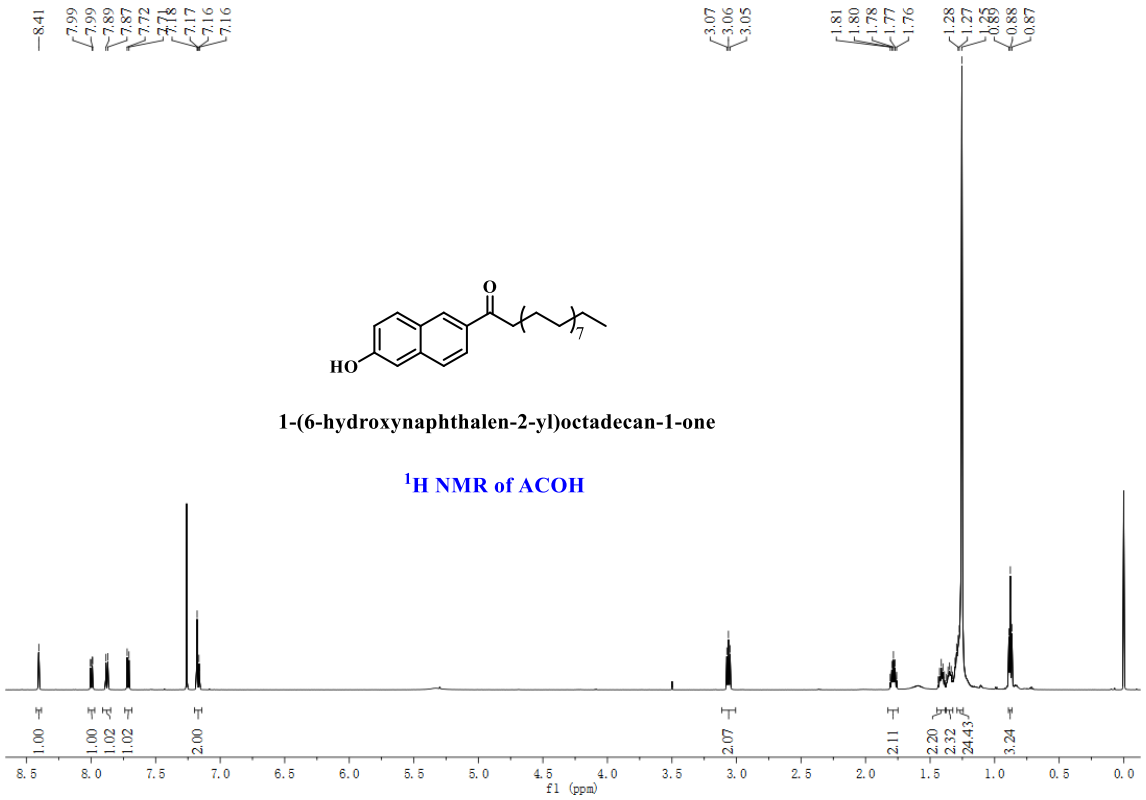

1-(6-hydroxynaphthalen-2-yl)octadecan-1-one

^{1}H NMR of ACOH

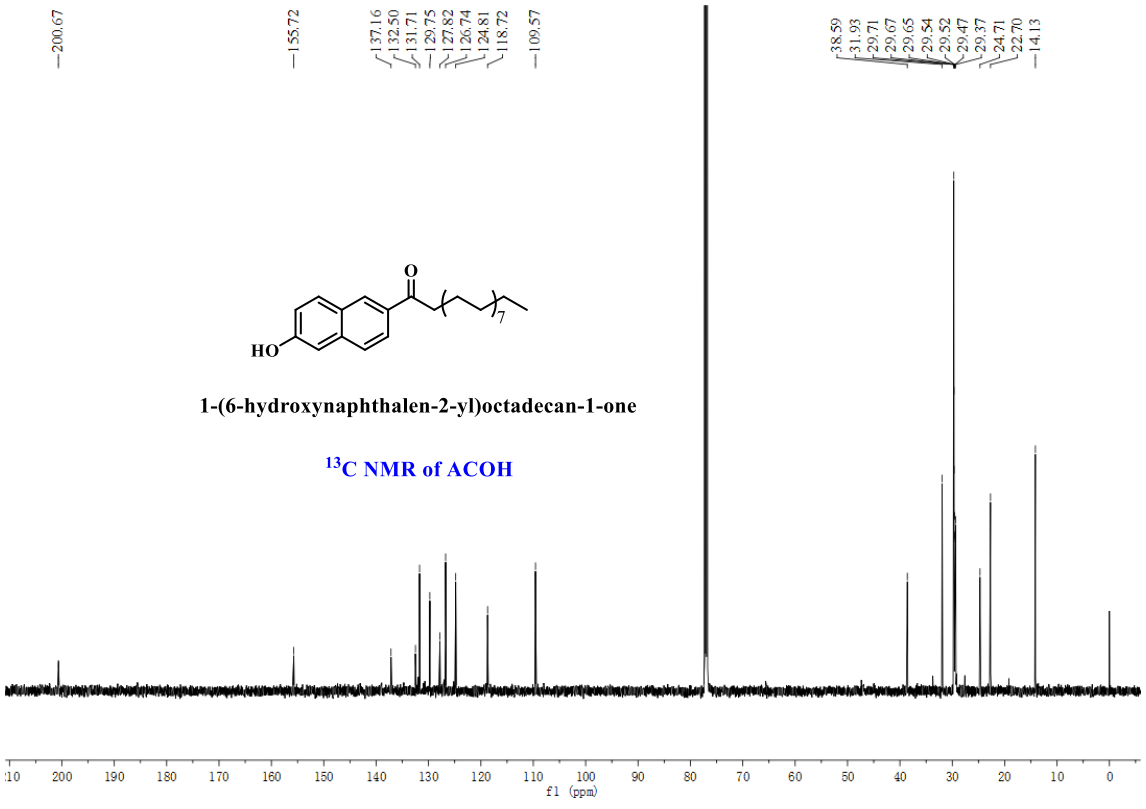

1-(6-hydroxynaphthalen-2-yl)octadecan-1-one

^{13}C NMR of ACOH

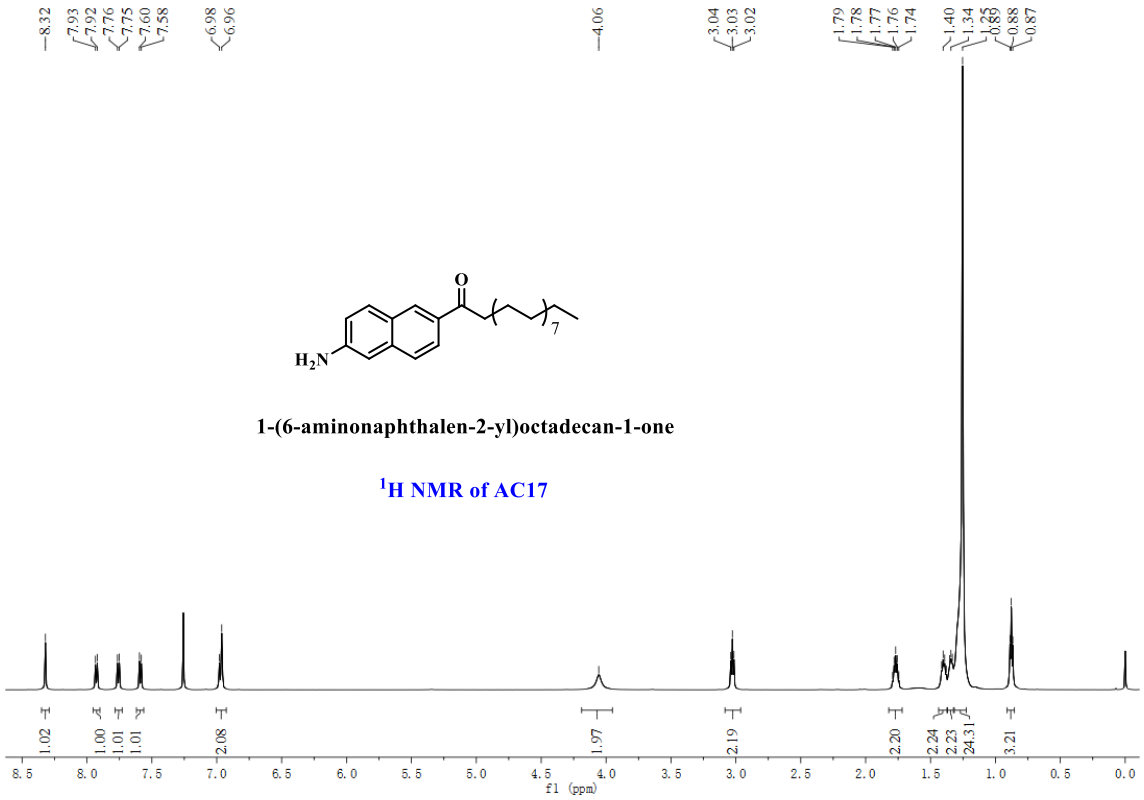

1-(6-aminonaphthalen-2-yl)octadecan-1-one

^{1}H NMR of AC17

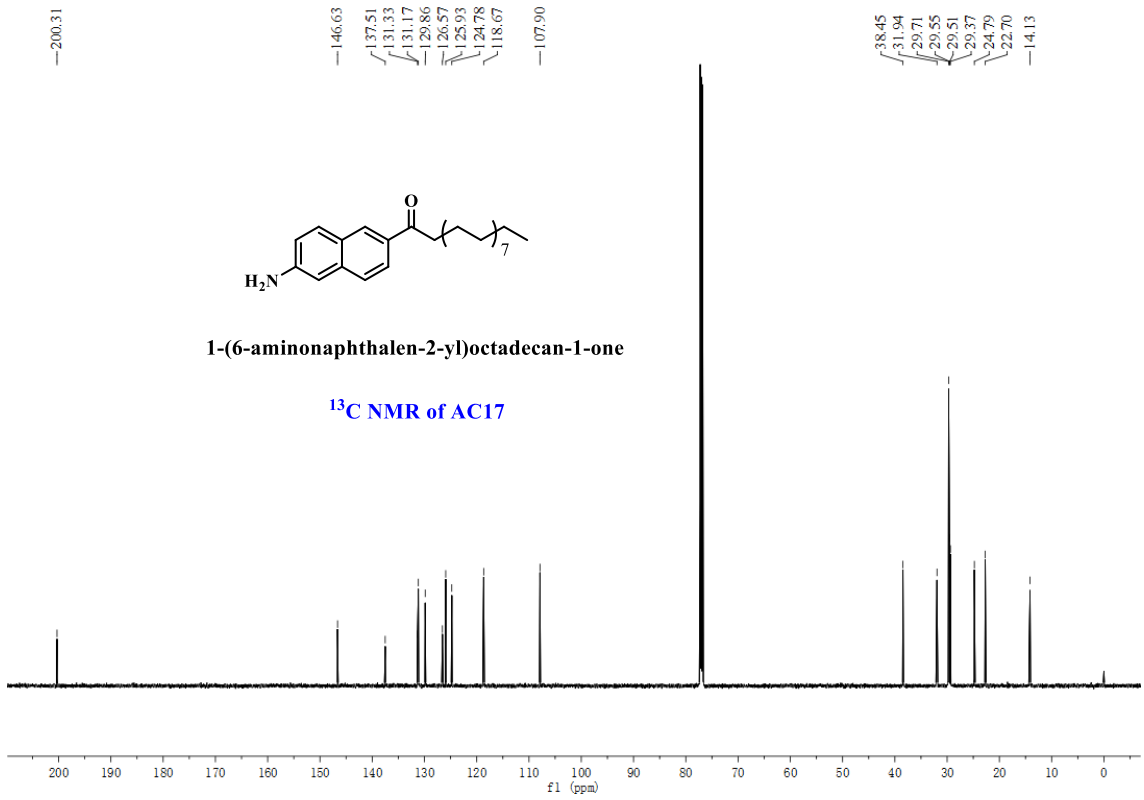

1-(6-aminonaphthalen-2-yl)octadecan-1-one

^{13}C NMR of AC17

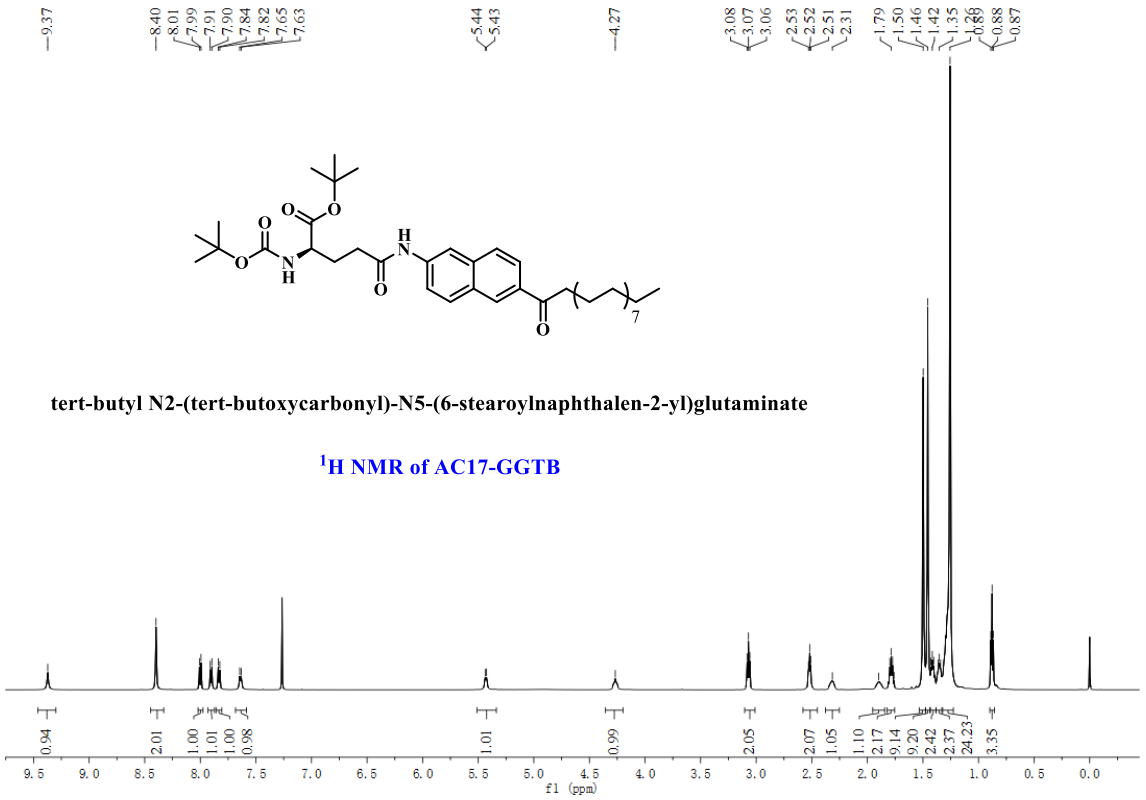

tert-butyl N2-(tert-butoxycarbonyl)-N5-(6-stearoylnaphthalen-2-yl)glutaminate

^{1}H NMR of AC17-GGTB

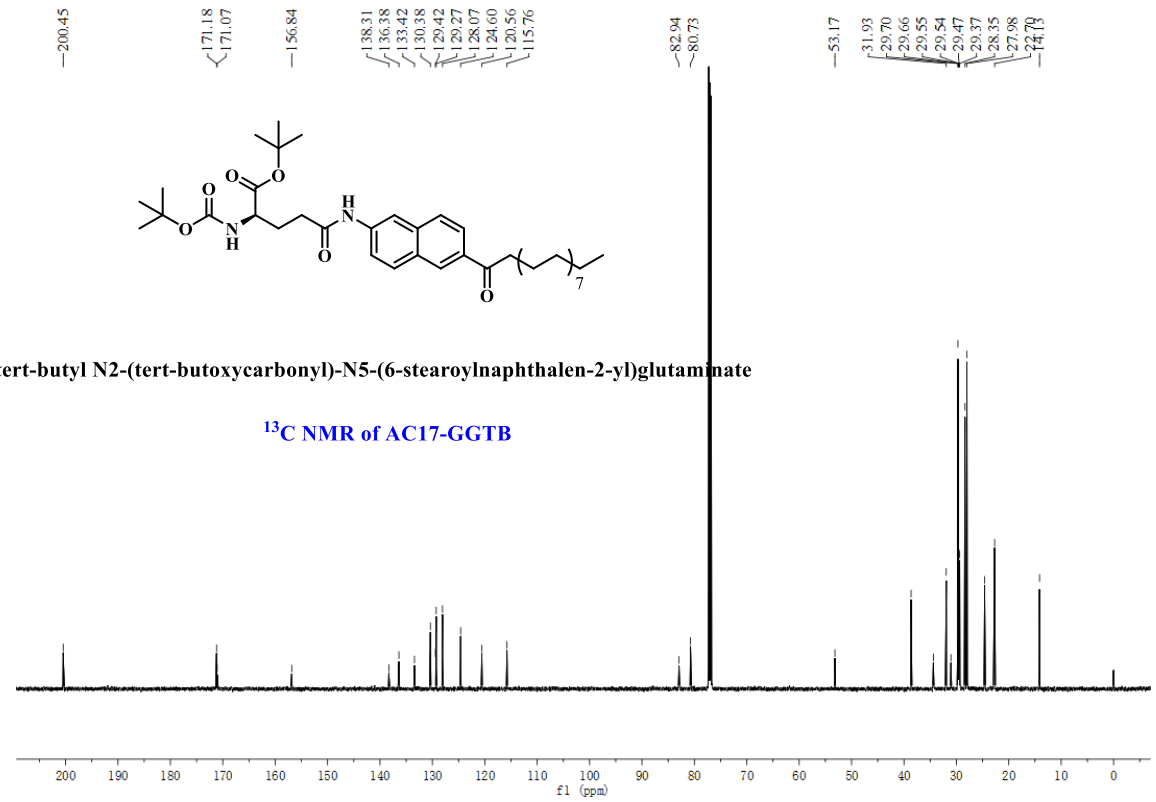

tert-butyl N2-(tert-butoxycarbonyl)-N5-(6-stearoylnaphthalen-2-yl)glutaminate

^{13}C NMR of AC17-GGTB

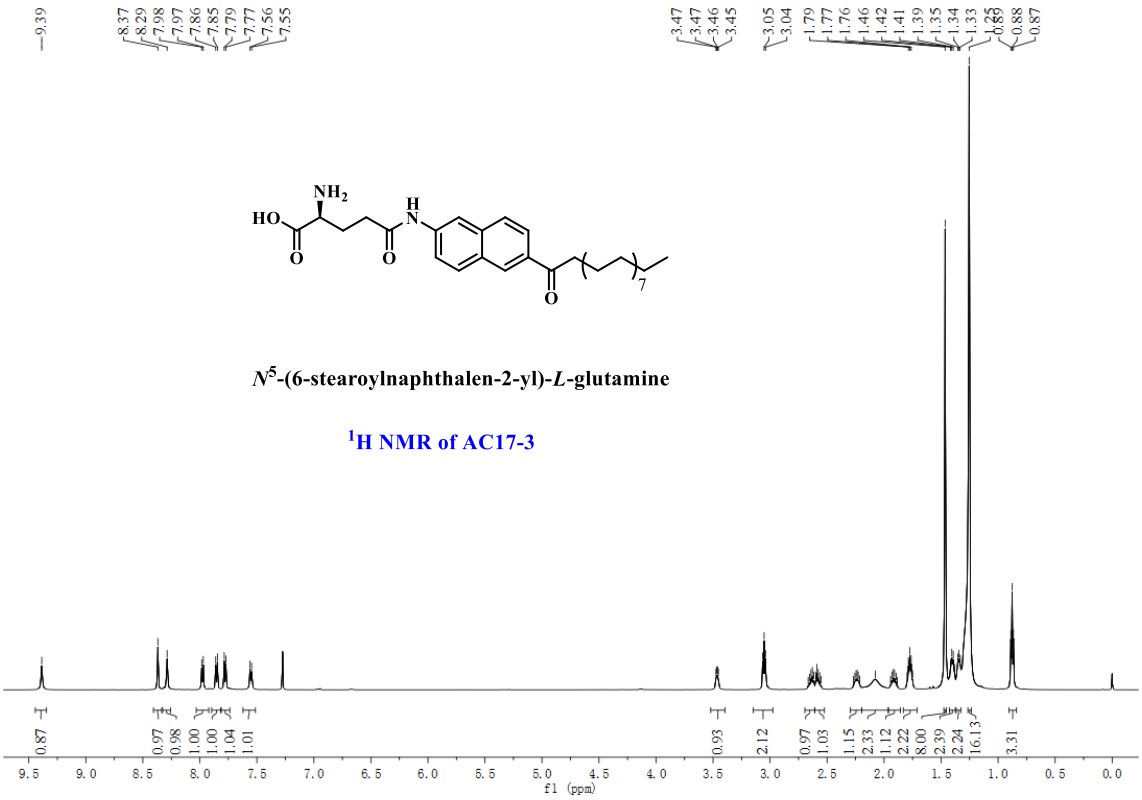

N^5-(6-stearoylnaphthalen-2-yl)-*L*-glutamine

^{1}H NMR of AC17-3

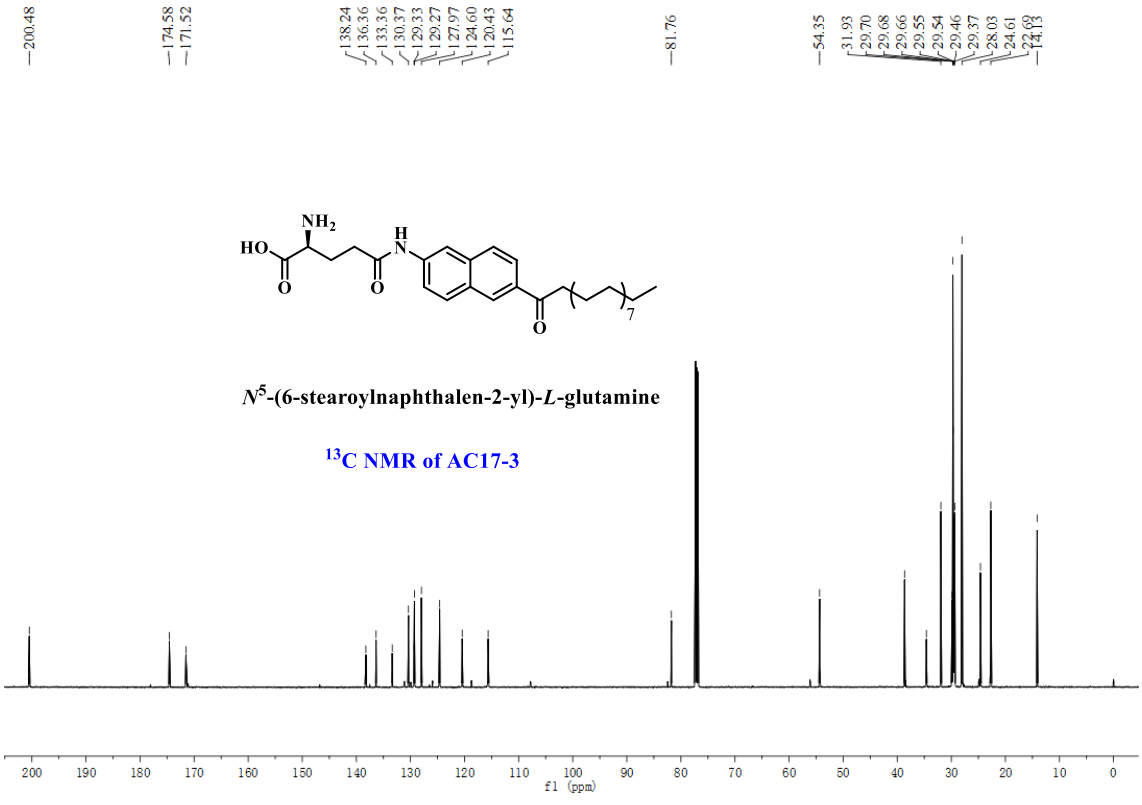

N^5-(6-stearoylnaphthalen-2-yl)-*L*-glutamine

^{13}C NMR of AC17-3

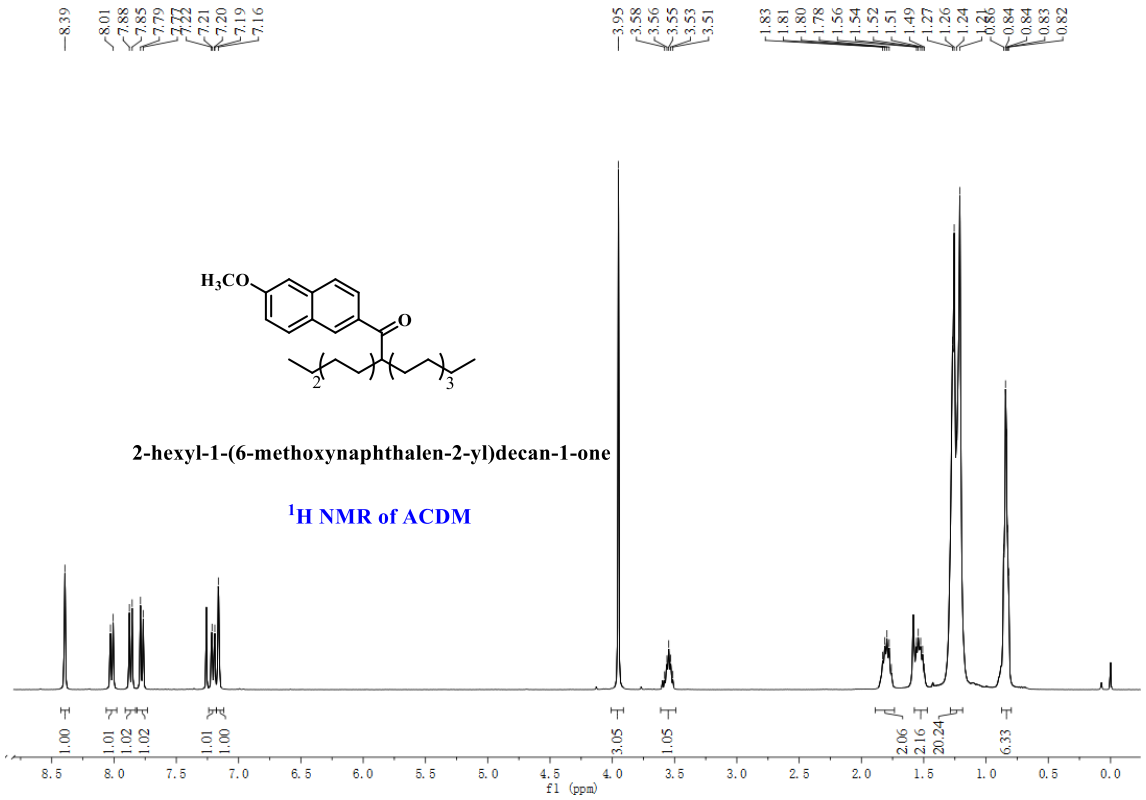

2-hexyl-1-(6-methoxynaphthalen-2-yl)decan-1-one

^{1}H NMR of ACDM

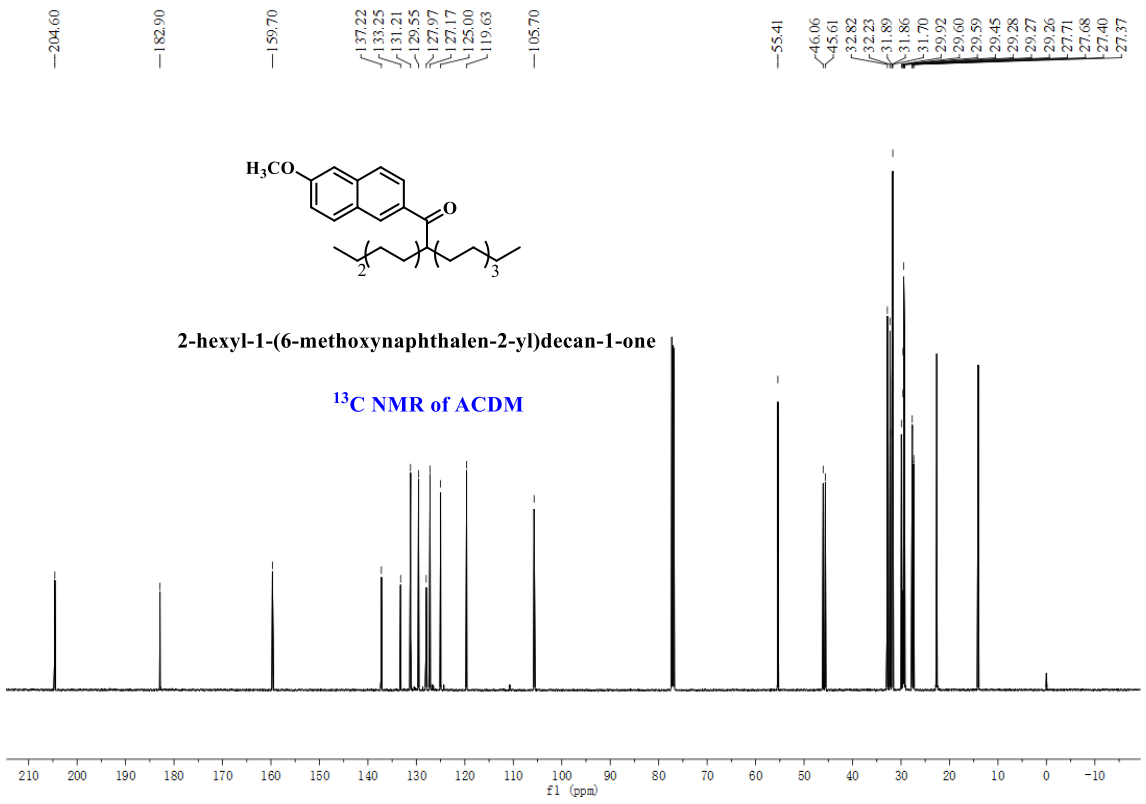

2-hexyl-1-(6-methoxynaphthalen-2-yl)decan-1-one

^{13}C NMR of ACDM

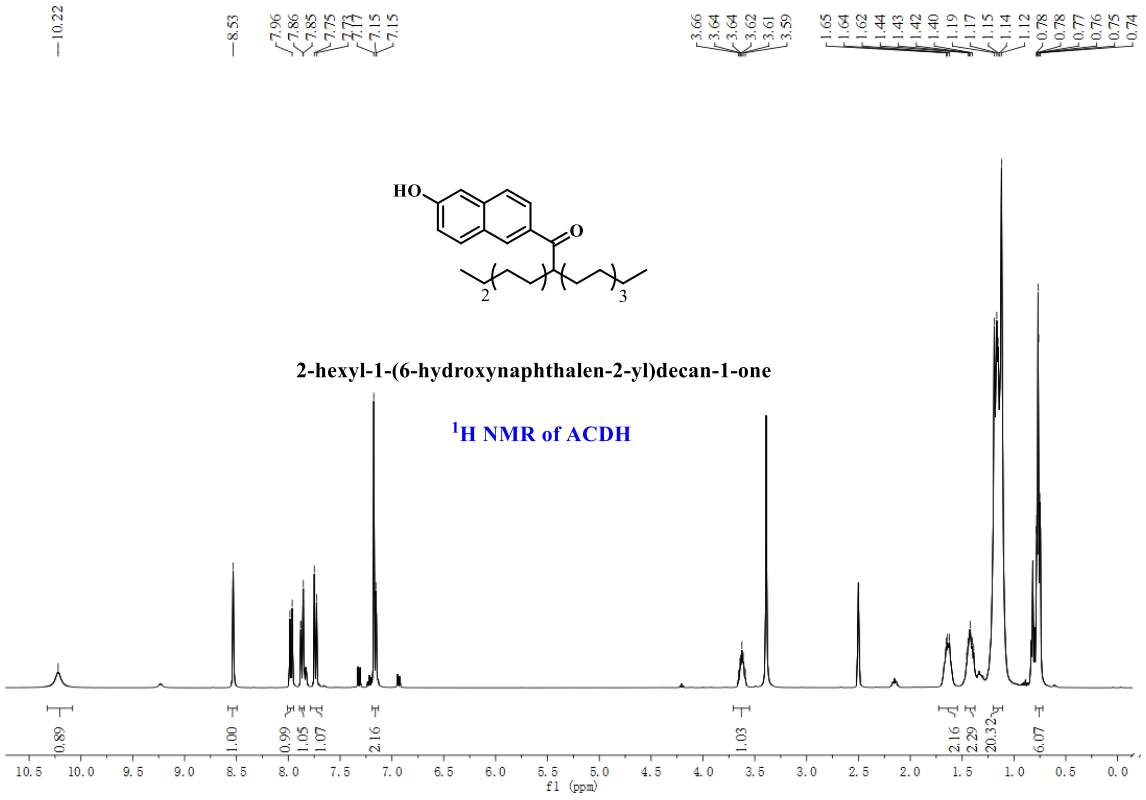

2-hexyl-1-(6-hydroxynaphthalen-2-yl)decan-1-one

^{1}H NMR of ACDH

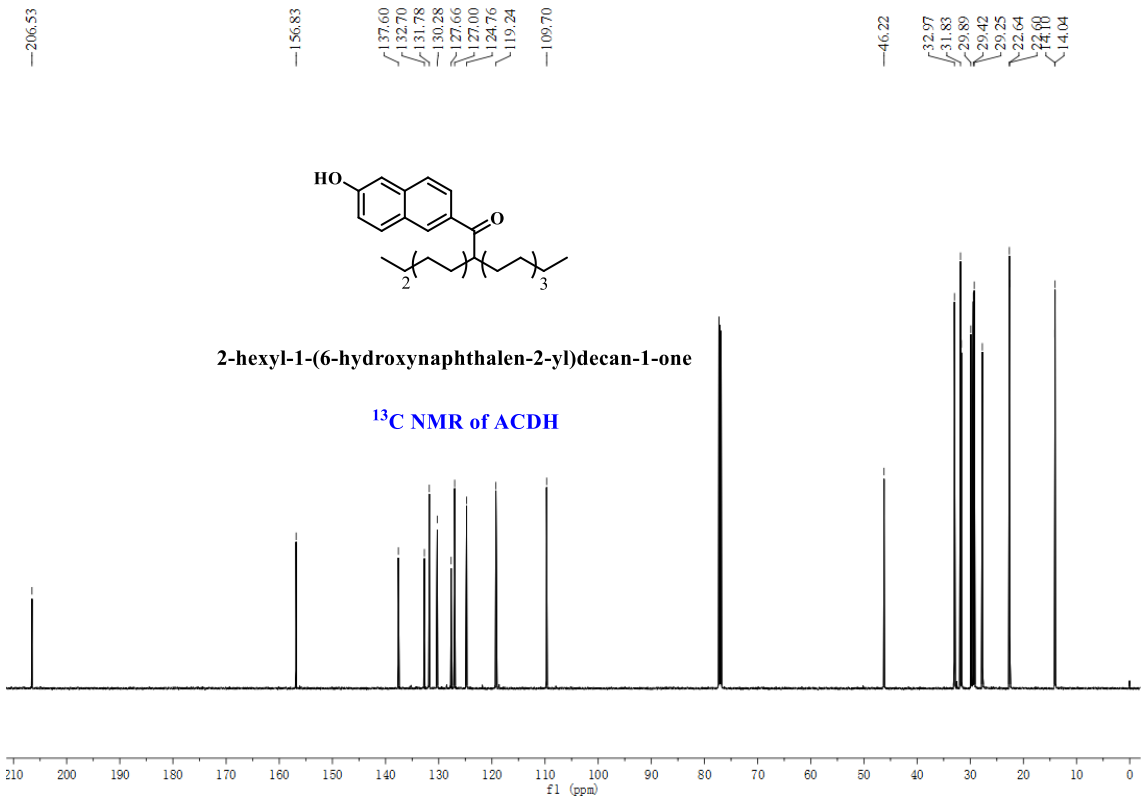

2-hexyl-1-(6-hydroxynaphthalen-2-yl)decan-1-one

^{13}C NMR of ACDH

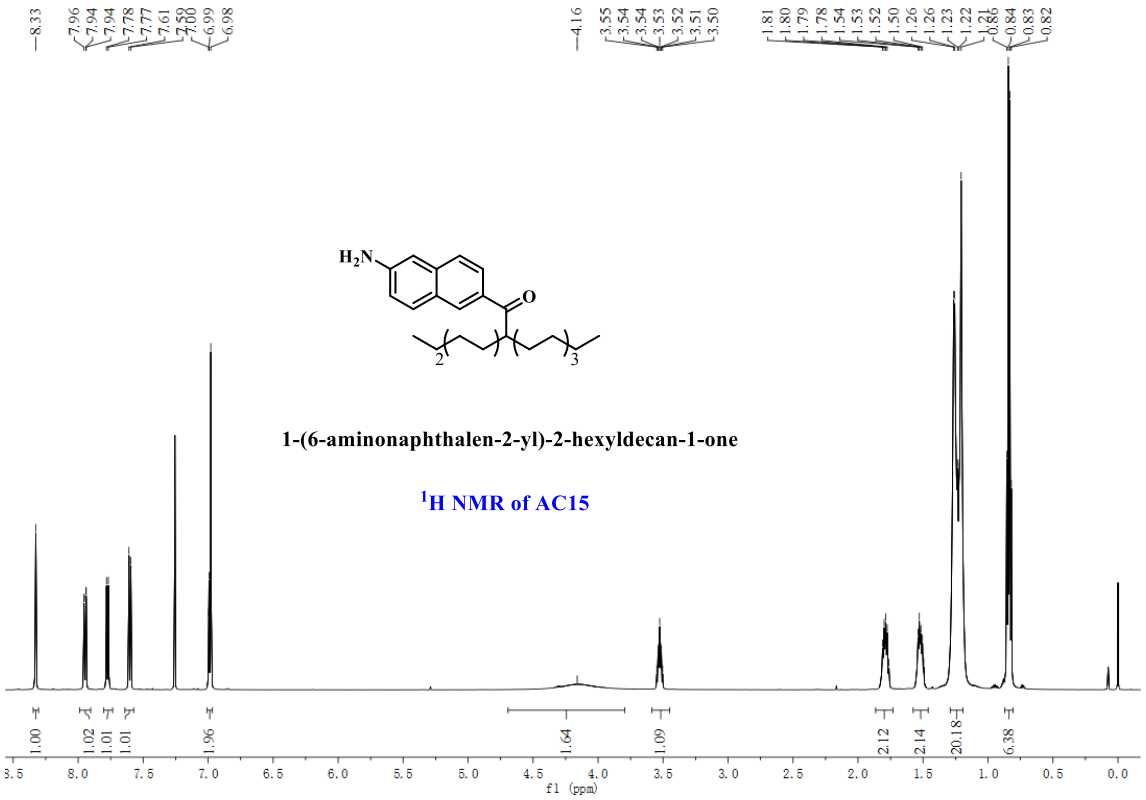

1-(6-aminonaphthalen-2-yl)-2-hexyldecan-1-one

^{1}H NMR of AC15

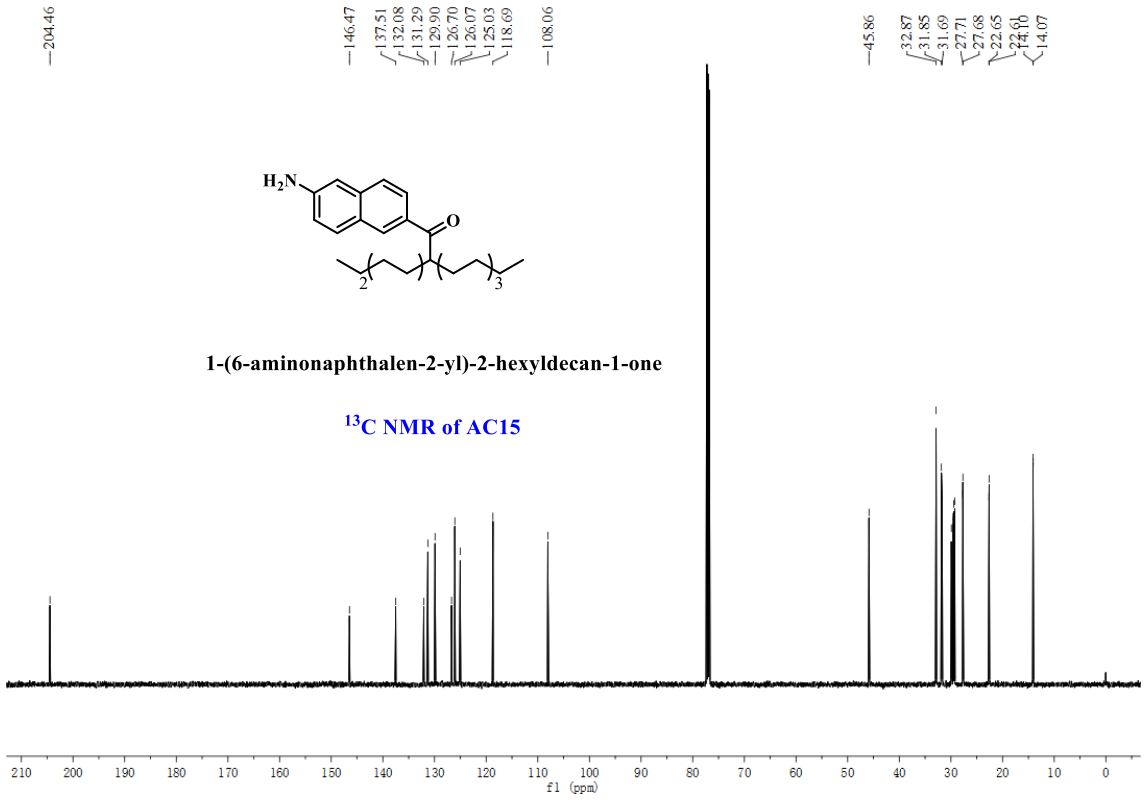

1-(6-aminonaphthalen-2-yl)-2-hexyldecan-1-one

^{13}C NMR of AC15

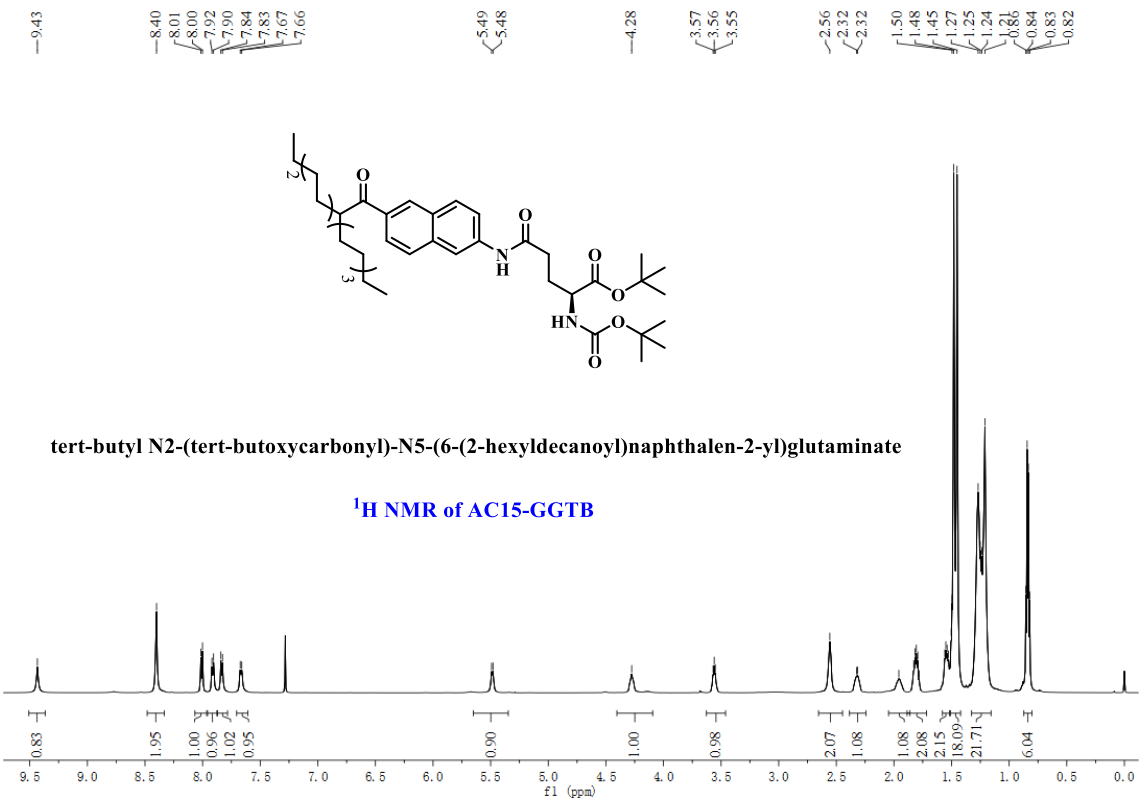

tert-butyl N2-(tert-butoxycarbonyl)-N5-(6-(2-hexyldecanoyl)naphthalen-2-yl)glutaminate

^{1}H NMR of AC15-GGTB

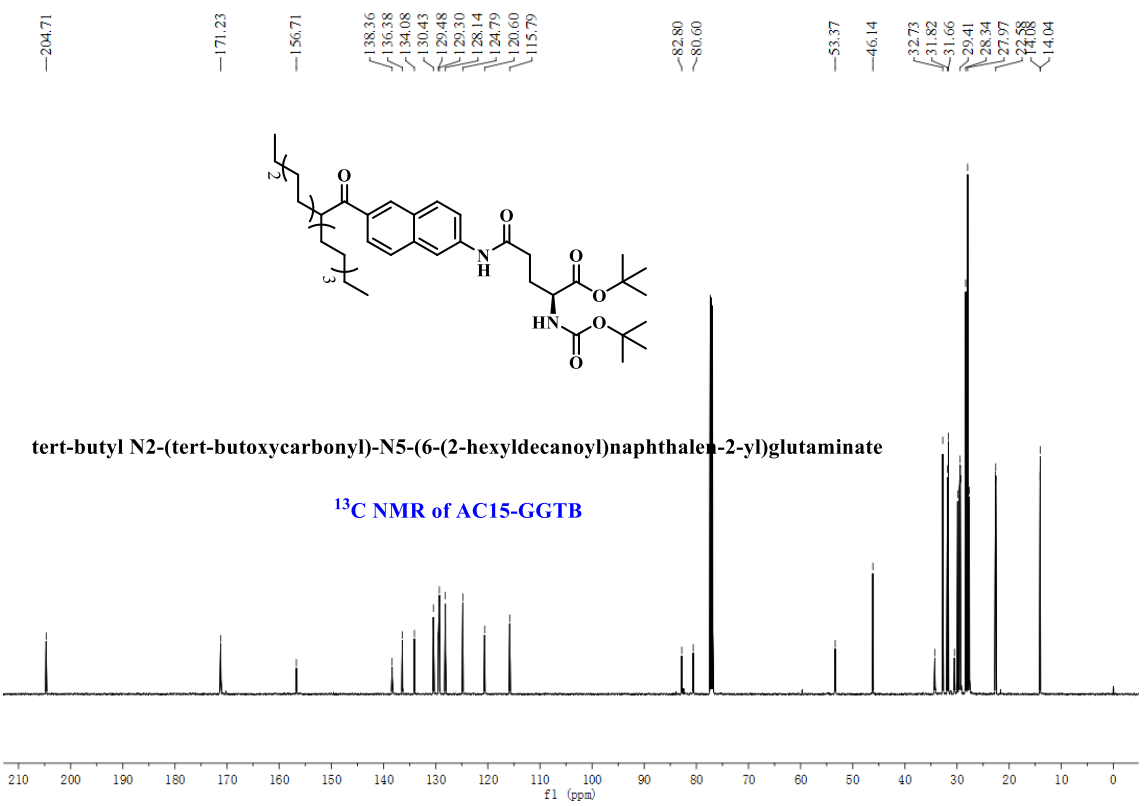

tert-butyl N2-(tert-butoxycarbonyl)-N5-(6-(2-hexyldecanoyl)naphthalen-2-yl)glutaminate

^{13}C NMR of AC15-GGTB

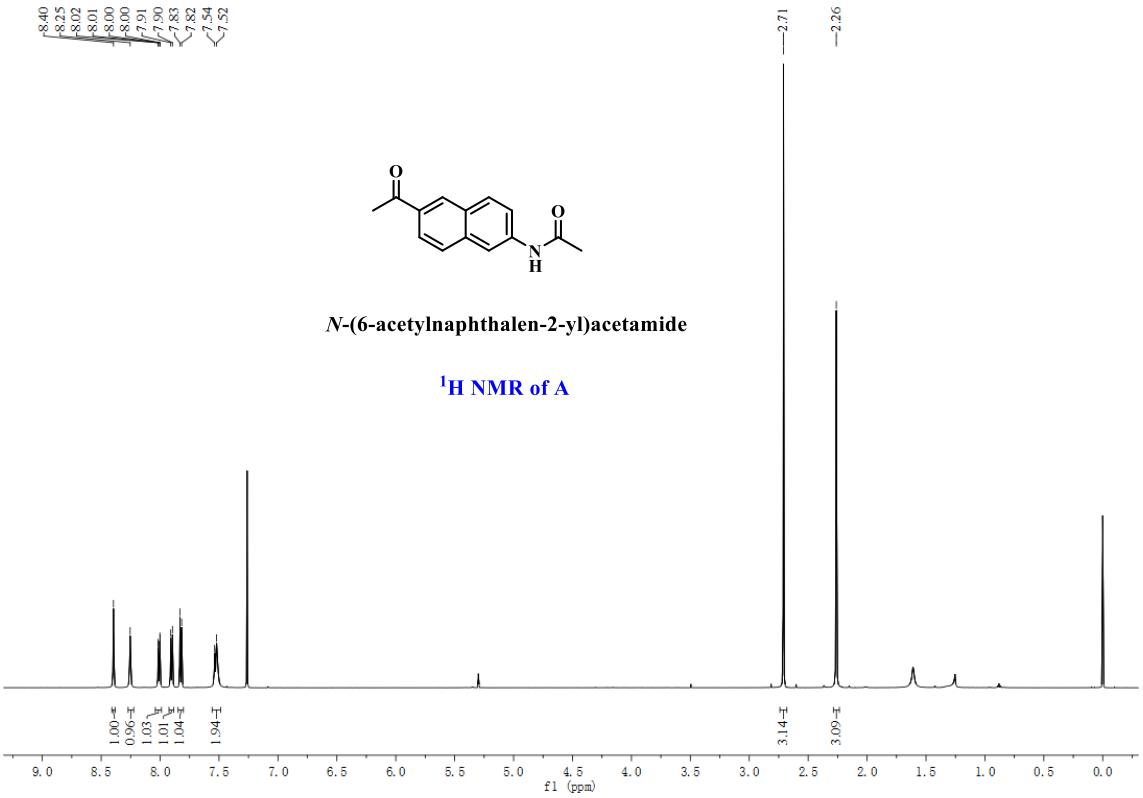

***N*-(6-acetylnaphthalen-2-yl)acetamide**

^{1}H NMR of A

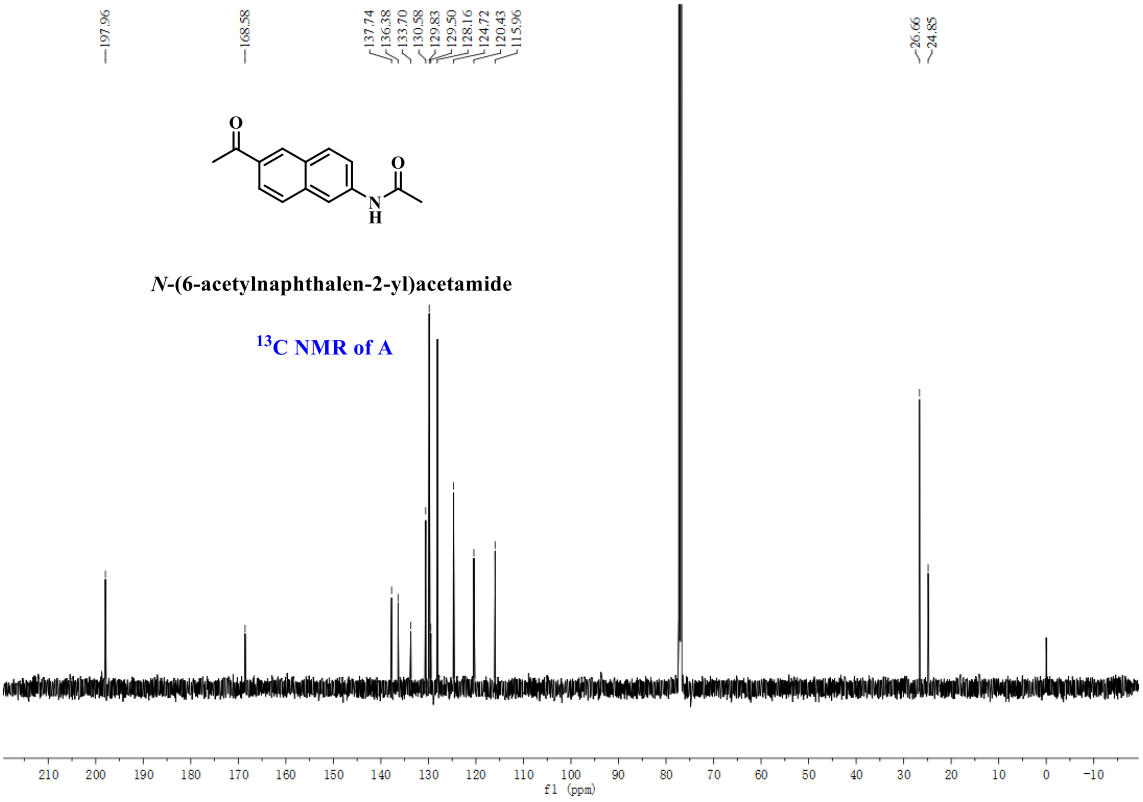

***N*-(6-acetylnaphthalen-2-yl)acetamide**

^{13}C NMR of A